Dear Editor,

We thank you for encouraging us to submit a revised version of our manuscript entitled:

Paleogeographic controls on the evolution of Late Cretaceous ocean circulation

Please find below the response to referee comments and the revised version of the manuscript. Please note that the response is identical to the author comments that we posted online in response to the reviewer comments.

Specifically, as you underlined in your online comment, the major criticism from Reviewer #1 concerned the treatment of atmospheric CO_2 levels in the Maastrichtian because reconstructions inferred from proxy records suggest lower concentrations in the latest Cretaceous than in the Cenomanian. In the revised manuscript, we know describe additional results from a Maastrichtian simulation performed with atmospheric CO_2 levels of 560 ppm (Section 4.3.5). Considering reduced CO_2 concentrations in the Maastrichtian allows an improvement of the model-data comparison of temperatures based on $\delta^{18}O$ records (Section 5.2.4) but does not change the conclusions of our manuscript. The simulated ocean circulation is indeed relatively insensitive to changes in CO_2 levels, at least in the range tested here (Section 5.1.2). We now also offer a broader discussion on the sensitivity of ocean circulation to atmospheric CO_2 levels (Section 5.1.2).

Reviewer #2 was mostly concerned with the length of the manuscript. Although we firmly believe that the length of our manuscript is a strength because the details of water mass pathways will probably be useful to both climate modelers and paleoceanographers, we have tried to keep Reviewer #2 comment in mind and have paid particular attention to improve readability and reduce length where possible. For instance, the comparison to Donnadieu et al. (2016) has been significantly reduced, as suggested. We have organized the paper into clear and intuitive sections and subsections, which can be conveniently skipped over if of less interest to the reader. This said, the manuscript is slightly longer than the previous version due to the addition of the 560 ppm Maastrichtian simulation in response to comments from Reviewer #1.

We have also improved the wording in several places and have corrected a major omission, which is that we incorrectly referred to the Indian Ocean in place of the Neotethys Ocean. In the Late Cretaceous, the Indian Ocean is restricted to the Southern Hemisphere below India whereas the ocean bathing Europe and the southern margin of Asia is the

Neotethys Ocean. Figures and calculations have been revised to take this new ocean distribution into account.

We are confident that this revised version meets the high scientific standards of Climate of the Past, and we believe that our manuscript will be a valuable and interesting contribution for a large audience in the paleoclimate community.

On behalf of all co-authors,
Sincerely yours,

Dr. Jean-Baptiste Ladant
Department of Earth and Environmental Sciences
University of Michigan
Ann Arbor, MI 48109, USA
Email: jbladant@umich.edu

Response to comments from Stuart Robinson (Referee #1)

I enjoyed reading this well-written paper that uses an Earth System model to explore the sensitivity of ocean circulation to long-term changes in Cretaceous palaeogeography by comparing simulations of Cenomanian and Maastrichtian conditions. This is an important and active area of research, as geochemical proxy records for Late Cretaceous ocean circulation (such as those from neodymium isotopes), although useful in documenting stratigraphic changes in local water mass chemistry, have proven harder to interpret unambiguously in terms of water mass sources and flow path. In this context modelling exercises are highly complementary and informative. I am certain this paper is appropriate for Climates of the Past.

Thank you for this comment.

My only significant issue with this paper is the treatment of CO2 levels and the comparison of the models with climate proxy records (Section 2.4).
The baseline simulations have CO2 set at 1120 ppm (4 times pre-industrial atmospheric levels, PAL), which is an entirely appropriate starting assumption for much of the Cretaceous, but as acknowledged (lines 981-993), was, in the latest Cretaceous, likely lower than in the mid-Cretaceous. It is surprising that no sensitivity analysis to CO2 levels has been included (especially as the same group has just published limited aspects of the model results, but including 2x and 4x simulations, in Haynes et al in press in Geology; https://doi.org/10.1130/G47197.1). The Haynes proxy and model results need to be included in the paper throughout, especially if they allow a consideration of how the sensitivity of the simulations to CO2 change.

Thank you for raising this question. We originally decided against including a sensitivity simulation to CO_2 in order to focus solely on the impact of paleogeography on Late Cretaceous ocean circulation. However, we agree that including a lower CO_2 Maastrichtian simulation allows the study to be more comprehensive. We have therefore revised the manuscript to add the 2x CO_2 simulation described in Haynes et al. (2020). Interestingly, the model shows limited sensitivity to CO_2 in terms of ocean circulation in that the pathways of intermediate and deep circulation are not noticeably modified. However, as described in Haynes et al. (2020), the lower CO_2 simulation does show a slightly more vigorous circulation. This low sensitivity of the Cretaceous ocean circulation to CO_2 is consistent with the results of Donnadieu et al. (2016) and the simulations of Farnsworth et al. (2019) with small exceptions (but see our response to next comment).

New sections devoted to the analysis and discussion of the lower CO_2 simulation can be found in the revised manuscript (sections 4.3.5, 5.1.2, 5.2.4).

Finally, the new Pacific datasets reported by Haynes et al. (2020) were already used in the original version of the manuscript. Please refer to Tables S3 and S4 (previously Tables S2 and S3) and Fig. 13.

The results at 4xPAL show substantial differences in the pattern of ocean circulation to those reported by Donnadieu et al (2016). It is suggested (lines 740 onwards) that this might be due to the more complex nature of CCSM and the role of continental run off in these different models. However, other model simulations (not discussed in the paper) have suggested that CO2 plus palaeogeographic change may be significant effects on ocean circulation at various times. in particular, Farnsworth et al (2019) in GRL highlight that in their Maastrichtian simulation using HadCM3 ocean circulation is extremely sensitive to CO2, with a switch between South Pacific deep-water production at 4xPAL to South Atlantic deep-water production at 2xPAL. It would be good if the authors could include some discussion of the results of Farnsworth et al. (2019) and their thoughts on the significance of the Farnsworth result.

We focused the comparison to previous model simulations to that of Donnadieu et al. (2016) because this study is the only one providing a detailed analysis of the reorganizations of deep ocean fluxes in the Late Cretaceous. Farnsworth et al. (2019) indeed report a strong sensitivity to CO_2 in their Maastrichtian simulation (with a shift in deep-water formation regions), but this strong sensitivity only occurs twice across all the simulations performed by Farnsworth et al. (2019) whereas the ocean circulation in all the other simulations is relatively insensitive to CO_2.
Whether this sensitivity is due to the specific Maastrichtian (~ 68.2 Ma, as per Lunt et al. 2016) and Selandian (~ 60.6 Ma) paleogeographies or to something else is unclear because Farnsworth et al. (2019) do not enter details as to what causes this response in the HadCM3BL-M2.1aD earth system model. What is even more intriguing is that if specific details of the Maastrichtian and Selandian paleogeographies are responsible for this model behavior then why is the Danian (~ 63.9 Ma) not producing the same behavior given that this stage occurs between the Maastrichtian and the Selandian? One possible answer might be provided by the model setup of the simulations of Lunt et al. (2016), of which the simulations in Farnsworth et al. (2019) are extensions. Table 1 of Lunt et al. (2016) shows that different smoothing had to be applied to the Maastrichtian, Danian and Selandian simulations to ensure model stability. For instance, the Maastrichtian simulation has a flat polar Southern Ocean, whereas the Danian and Selandian have not. In the absence of a specific analysis about the role of CO_2 on ocean circulation in the Maastrichtian simulations of Farnsworth et al. (2019), we can only speculate that these changes might be partly caused by the variable high-latitude smoothing applied.

We have added the following discussion about Farnsworth et al. (2019) results (in section 5.1.2 of the

revised manuscript):

"Ocean circulation is mostly insensitive to reducing the atmospheric CO_2 concentrations in our Maastrichtian configuration. The intermediate and deep water mass pathways are identical although the intensity of the water fluxes across major oceanic gateways is slightly enhanced in the 2x CO_2 simulation (Haynes et al., 2020). This insensitivity of Late Cretaceous ocean circulation to CO_2 levels is consistent with the results of Donnadieu et al. (2016), which shows that Late Cretaceous simulations performed at 2x, 4x and 8x CO_2 PAL predict similar areas of deep-water formation. In contrast, Farnsworth et al. (2019) recently reported that reducing atmospheric CO_2 levels from 4x to 2x in a Maastrichtian configuration in the HadCM3BL-M2.1aD earth system model led to a shift in deep-water formation area from the South Pacific Ocean to the South Atlantic and Indian Oceans. This high sensitivity to CO_2 only occurs in the Maastrichtian simulation among all the 12 Cretaceous simulations (one per Cretaceous stage) performed by Farnsworth et al., and occurs again only once (in the Selandian stage, ~ 60.6 Ma) among all their 7 Paleogene simulations. In the other simulations, both the 2x and 4x CO_2 simulations predict similar areas of deep-water formation. The temporal proximity of the Maastrichtian and Selandian stages led Farnsworth et al. (2019) to suggest that the time period close to the Cretaceous/Paleogene boundary might be particularly sensitive to atmospheric CO_2 but it is not clear in this case why their simulation of the Danian stage (~ 63.9 Ma) does not exhibit a similar behavior. As Farnsworth et al. (2019) do not provide a detailed analysis of ocean circulation changes in the Maastrichtian and Selandian stages relative to the others, we can only speculate that these changes might be partly caused by high-latitude smoothing, which is performed on the simulations to ensure model stability and which varies between stages (Lunt et al., 2016; Farnsworth et al., 2019)."

In addition, we provide a discussion on the role of CO_2 on ocean circulation from a wider perspective (also in section 5.1.2 of the revised manuscript):

"More generally, the impact of atmospheric CO_2 levels on ocean circulation has been shown to significantly vary in past greenhouse climate modeling work (Poulsen et al., 2001; Lunt et al., 2010; Poulsen and Zhou, 2013; Donnadieu et al., 2016; Hutchinson et al., 2018; Farnsworth et al., 2019; Zhu et al., 2020). The causes for this large spread in results may be diverse and are difficult to isolate but we hypothesize that the model climate sensitivity to CO_2 and the range of atmospheric CO_2 levels investigated could explain such variability. Winguth et al. (2010) report results of Paleocene-Eocene Thermal Maximum (PETM) simulations using the CCSM3 fully-coupled model (with the CAM3 atmospheric model) and show that ocean circulation and deep-water formation areas remain similar regardless of CO_2, although the intensity of overturning decreases with increasing CO_2. More recently, Zhu et al. (2020) report results of PETM simulations performed at 1x, 3x, 6x and 9x CO_2 PAL using the CESM1.2 ESM (with the CAM5 atmospheric model) and document a shift in deep and intermediate water formation areas between 1x and 3x CO_2 and complete cessation of deep-water formation at 6x and 9x CO_2. The climate sensitivity of CESM1.2 has been shown to be greater than

that of CCSM3, and, contrary to CCSM3, to increase with background CO_2 levels (Zhu et al., 2019). Earth System Models with high climate sensitivity to CO_2 may demonstrate a higher sensitivity of ocean circulation to CO_2 because the climate state in which the radiative forcing of CO_2 leads to a warming sufficient to stop deep-water formation can be expected to occur for smaller changes in atmospheric CO_2 levels."

Section 2.4 compares proxy temperature records with the simulations and finds (line 981) a disagreement, which the authors relate to the constant CO2 value used. Given this major assumption in the simulations presented, I think that much of the oxygen isotope discussion in section 2.4 is either irrelevant or should be prefaced by the caveat that CO2 does not vary in the simulations and, therefore, the temperatures (and temporal evolution of temperature) in the model simulations is unlikely to match the proxy records. The conclusion to this section (lines 1014-1016) raises the question of whether Section 2.4 is necessary.

The aim of this section was to compare proxy temperature records with the change in temperature between the Cenomanian and Maastrichtian to investigate whether part of the proxy temperature change could be explained by paleogeography-driven changes in ocean circulation and whether the temperature change driven by gateways change could help provide additional constraints on the configuration of the gateways.

We fully agree that many discrepancies were expected, as the CO_2 did not vary in the simulations and because the temperature changes driven by deepening of gateways was smaller than the Cenomanian-Maastrichtian change.

Because we now include the lower CO_2 Maastrichtian simulation, we have also revised this section (section 5.2.4 of the revised manuscript). In short, the comparison between proxy temperature records and model results including the lower CO_2 Maastrichtian simulation shows better consistency. This is especially true for benthic records, whereas planktic records generally show larger amplitude of change, suggesting that regional deviations from the mean -1 ‰ seawater $\delta^{18}O$ may have played a significant role (e.g., Zhou et al. 2008, Zhu et al. 2020).

Minor issues/suggestions:

Use of past and present tense – in a number of places (e.g. line 149, 153), the present tense is used to describe events in the geological past.

Done.

Line 80-82: Odd structure to this sentence - consider rephrasing as: "This conjecture is corroborated

by studies of the temporal trends and spatial variations in neodymium (Nd) isotopes... a quasi-conservative tracer of waters masses...”

Thank you for the suggestion. It has been rephrased.

Line 83: insert commas before, and after, “in particular”

Done.

Line 84-85; papers led by Robinson should be included in this list as they were amongst the first to show the long-term shift in Nd between the mid and latest Cretaceous.

The Robinson papers should indeed not have been overlooked from this list. They have been added.

Line 86 onwards – I think it may also be worth mentioning here that another area of uncertainty is regarding palaeowater depth – some sites are rather poorly constrained and thus the possibility exists that different water masses are being sampled but considered as broadly of the same depth.

We fully agree and we thank you for the suggestion. The paleodepth issue is one of the reasons that led us to categorize water transports along a vertical axis. We have rephrased the sentence as:
“However, there is no consensus on the specific modes and evolution of ocean circulation across the Late Cretaceous as interpretation is complicated by the lack of Late Cretaceous ε_{Nd} records in key places and times, by the possibility of modification of ε_{Nd} values along flow paths, and by uncertainties in the paleodepth of sites where ε_{Nd} values were documented.”

Line 154: change to “black shale deposition”

Done.

Line 157: insert “the” before “South Atlantic”

Done.

Line 201: Insert “The” before “presence of a: : :”

Done.

Line 214-216: what is the reason for the shallower depth of the Drake Passage in the Maastrichtian versus the Cenomanian?

The paleogeographies of the two baseline Cenomanian and Maastrichtian simulations are those described in Lunt et al. (2016) and which have been given to the Lunt's group by Getech Plc. These datasets are proprietary and, while they can be used for scientific research, the underlying assumptions on particular paleodepths are not available. We used these datasets because the two baseline simulations are extensions of the Cenomanian and Maastrichtian simulations described in Tabor et al. (2016), which use the Lunt et al. (2016) paleogeographies.

Line 221: On the basis of results in Donnadieu, it is argued that the shallow depth differences in the Drake passage are not significant for global ocean circulation. However, given the differences in results overall, can the authors be certain that differences in depths <1000m will make no difference in their model framework?

We are confident that differences in depth < 1000 m in the Drake Passage in our Maastrichtian simulation would not lead to significant differences in the simulated ocean circulation. Indeed, the intermediate ocean circulation (500 – 1500 m) at the global scale is similar in the different Maastrichtian experiments (baseline + sensitivity) and we also note that the South Atlantic and South Indian/Tethys Ocean intermediate circulation is similar in the Cenomanian and the Maastrichtian baseline experiments, although the Cenomanian simulation has a deeper (800 m) Drake Passage. The similarity is the result of the persistence of deep convection in the South Pacific in the Cenomanian and in the various Maastrichtian experiments.
We acknowledge, though, that a ~ 1000 m deep Drake Passage could locally alter circulation patterns in the South Atlantic and/or eastern South Pacific Ocean, and as such, could make a difference in the interpretation of geochemical data. However, the influx of radiogenic Pacific waters into the South Atlantic is less consistent with ε_{Nd} trends and such a deep Drake Passage is also less consistent with tectonic evidence.

Line 279: replace "Indian" with "Tethyan"

Done.

Line 293: comment on why Sewall is used rather than Tabor.

The dynamic vegetation model of Tabor et al. (2016) produced low vegetation density at high latitudes that did not agree well with fossil-based reconstructions. As a result, simulated high latitude land

surface temperatures tended to be too cold and seasonally variable. Switching to prescribed vegetation, based on Sewall et al. (2007), helped reduce this temperature bias. Prescribed vegetation means that the distribution of plant functional types cannot change through time but plant phenology is still predicted by the model.
We have added these details in the revised version (in section 3 of the revised manuscript).

Line 330-332: Awkward sentence structure – consider rephrasing.

The sentence was changed as follows:
"Simulated changes in ocean circulation between the Cenomanian and the Maastrichtian and between the Maastrichtian and the sensitivity experiments are then compared to previous modeling studies and geochemical data."

Lines 356-357: small scale regional features of the simulations are described but the use of "South America" as the geographic descriptor is a bit too vague – please be more precise when describing where these local oceanographic features occur.

Done. We have added details in this paragraph, which now reads:
"Other low salinity coastal waters are found at equatorial latitudes in enclosed epicontinental basins on the eastern coast of West Africa (Saharan epicontinental sea) and on the northwestern coast of South America as well as in the isolated high-latitude basin located between Australia and Antarctica. In contrast, high salinity waters are found in enclosed subtropical basins, such as on the western coast of South America and on the Asian margin of the Neotethyan Ocean as well as in the Gulf of Mexico (Fig. 3B). These high salinity areas correlate with regions of high temperature, low river freshwater input and largely negative PME (Fig. 3A-D)."

Line 436: replace "to the subpolar" with "with the subpolar"

Done.

Line 437: insert "of" before "the South Atlantic"

Done.

Line 522: insert comma after "experiment" and delete "and"

Done.

Lines 760-771: This paragraph contains a lot of fundamental, introduction-level material about Nd-isotopes that might be better worked into the introduction to the paper rather than included in the discussion.

This paragraph has been moved to the introduction, as suggested.

Line 796: Robinson and Vance should be included in the citations here.

Done.

Line 819-824: I don't really see the justification for suggesting that the deep-waters exported from the Pacific in the Cenomanian were relatively low in eNd given that the values shown from the Pacific in Haynes et al (in press) suggest the south Pacific had relatively high eNd values (>-6) in the Maastrichtian, and, if the simulations are correct, probably the Cenomanian too. Given the relatively unradiogenic values of the eastern Australian coast and Ross Sea, is it not surprising that the Pacific data have values of >-6 in the Maastrichtian, if those regions are the source of the water masses? This section seems to be at odds with aspects of Haynes et al and the actual Cenomanian values of Indian and Atlantic water masses.

Thank you for this interesting question.
In our model, deep-water formation indeed occurs in the South Pacific high latitudes (> 60°S) but Haynes et al. (2020) (hereafter H2020) South Pacific sites are located in the low latitudes (~ 5°S for Mid-Pacific Mountains site 463 and ~ 10°S for Ontong-Java Plateau Site 1186), which makes a significant difference in terms of water mass pathway.
In both the Cenomanian and Maastrichtian simulations, deep waters formed in the high-latitude South Pacific mostly flow away from the Pacific Ocean following a westward current along the Australian margin (Fig. 7 and 11). Some of these sinking waters fill the eastern Pacific sector of the Southern Ocean. The deep tropical South Pacific, as well as the deep equatorial and North Pacific, are bathed by a mixture of recirculated deep waters from the Indian/Neotethyan Ocean (Fig. 7 and 11) and of deep waters from the deep eastern part of the Pacific sector of the Southern Ocean. Figure R1 shows the water mass age at 2900 m (roughly the depth of site 1186) in the South Pacific and the red star denotes the estimated position of site 1186. Water mass ages are likely not fully equilibrated in our simulations (see discussion in section 3 of the revised manuscript) but it can be seen that the waters bathing site 1186 are much older (> several centuries) than waters that have sunk in deep-water formation areas. It is reasonable to assume that the ε_{Nd} signature of these waters may have shifted toward higher Pacific-like values. This reasoning is also true for site 463 (Fig. R2).

These results are not at odds with H2020 because the 2x CO_2 Maastrichtian simulation of H2020 shows a more intense, yet similar, ocean circulation, which allows less time for sediment/water interaction than in the less intense 4x CO_2 Maastrichtian circulation. Consequently, the faster overturning may drive a smaller shift from the unradiogenic values of the source region (Australian coast/Ross Sea) to radiogenic Pacific values, which could explain the negative excursion in ε_{Nd} at the low latitude Pacific sites.

Line 825-827: Would it be possible to test the effect of imposing barriers in the Southern Tethys (around Kerguelen, I would imagine), even if they are not very well constrained?

Yes, it would be possible to raise bathymetric barriers in the Southern Tethys but it would require a significant amount of computing resources because the CESM model is complex and relatively high-resolution. We keep this interesting idea in mind for potential future experiments.

Lines 842 onwards. The Soudry data is incorporated into the discussion of Cenomanian circulation in the Tethys, yet, on line 846, it is stated (correctly) that the Soudry data come from neritic settings so cannot be used to interpret intermediate or deepwater circulation. Thus, it seems misleading (and a bit confusing for those unfamiliar with the datasets) to discuss Soudry if the conclusion (line 847) is that the data from neritic settings cannot be used to support the simulations.

The Soudry data are consistent with our Cenomanian simulations in that the model simulates strong westward currents through the Tethyan Ocean. We agree however that these data were awkwardly used in the original manuscript. Because of their limited relevance to our interpretation, we have removed the reference to Soudry et al. (2006) and Pucéat et al. (2005). This section now reads:
"Records from the equatorial Pacific (Murphy and Thomas, 2012) shows moderately high ε_{Nd} values (> –6) from the Cenomanian onwards. In addition, modern compilations of the ε_{Nd} signature of the continental margins in the eastern Mediterranean Sea (Ayache et al., 2016) and on the northeastern coast of Africa (Jeandel et al., 2007) indicate relatively radiogenic ε_{Nd} values (> –6). Inputs of radiogenic intermediate and deep waters from the Pacific into the North Atlantic via this Neotethyan pathway, regardless of whether sediment/water exchange in the Neotethyan Ocean may have contributed to their isotopic composition, provides a possible explanation for the ε_{Nd} signature of the deep North Atlantic (Fig. 13), which has more radiogenic values than the nearby North American and North African continents (Jeandel et al., 2007)."

Line 857: replace "and that: : :" with either "that: : :" or "but we are unable to exclude them."

The sentence was rephrased as:

"However, other events may also have contributed to raising the ε_{Nd} values of North Atlantic intermediate and deep waters."

Lines 875-881: Whilst I agree that boundary exchange could be an issue for the eNd data from Demerara Rise, the existence of very saline waters (based on the Mg/Ca and d18O data of Friedrich et al., 2008) do point to local formation of warm saline bottom waters and suggests that this feature of ocean circulation is missing in all model simulations.

This is correct and we mention that the model does not produce low-latitude intermediate or deep-water formation at Demerara Rise. However, we have modified the last part of this subsection to better emphasize the possibility that models might be unable to form low latitudes deep-water formation because of some missing processes and/or details of the local paleogeography. The new sentence reads:
"Our model results support boundary exchange as an explanation for very low Demerara Rise values but we cannot exclude the possibility that climate models are unable to reproduce low-latitude intermediate or deep-water formation at Demerara Rise because of missing processes or insufficiently detailed local paleogeography."

Line 890: The papers by Robinson support increased exchange by, and during, the Maastrichtian and should be cited here.

We have corrected this oversight.

Line 910-912: One important consideration could also be the significance of palaeowater depth differences and variable amounts of boundary exchange between sites (and through time) and the effect these factors might have on the records of eNd. Furthermore, the use of different archives of eNd, could also be a source of offsets between different datasets.

We agree and now hint at these considerations in the introductory section about Neodymium isotopes (section 5.2.1). The last two paragraphs now reads:
"All of these hypotheses explain the similarity in deep-water εNd values between the North Atlantic, South Atlantic and Indian Oceans in the Maastrichtian (Fig. 13) by greater communication between the basins (Robinson and Vance, 2012; Murphy and Thomas, 2013; Moiroud et al., 2016). Other records instead suggest that bathymetric barriers of the Rio Grande Rise (RGR) – Walvis Ridge (WR) system in the South Atlantic prevented deep north-south flow between the North Atlantic and the Southern Ocean until the Paleogene (Voigt et al., 2013; Batenburg et al., 2018) although recent work suggest that deep channels existed through the RGR-WR system in the Late Cretaceous (Moiroud et

al., 2016; Pérez-Díaz and Eagles, 2017).

The opening of the Atlantic and Southern Ocean nonetheless played a major role in the convergent evolution of εNd values in the Late Cretaceous by affecting intermediate and deep flow patterns as well as the residence time of water masses and, hence, local εNd inputs such as boundary exchange."

Figures

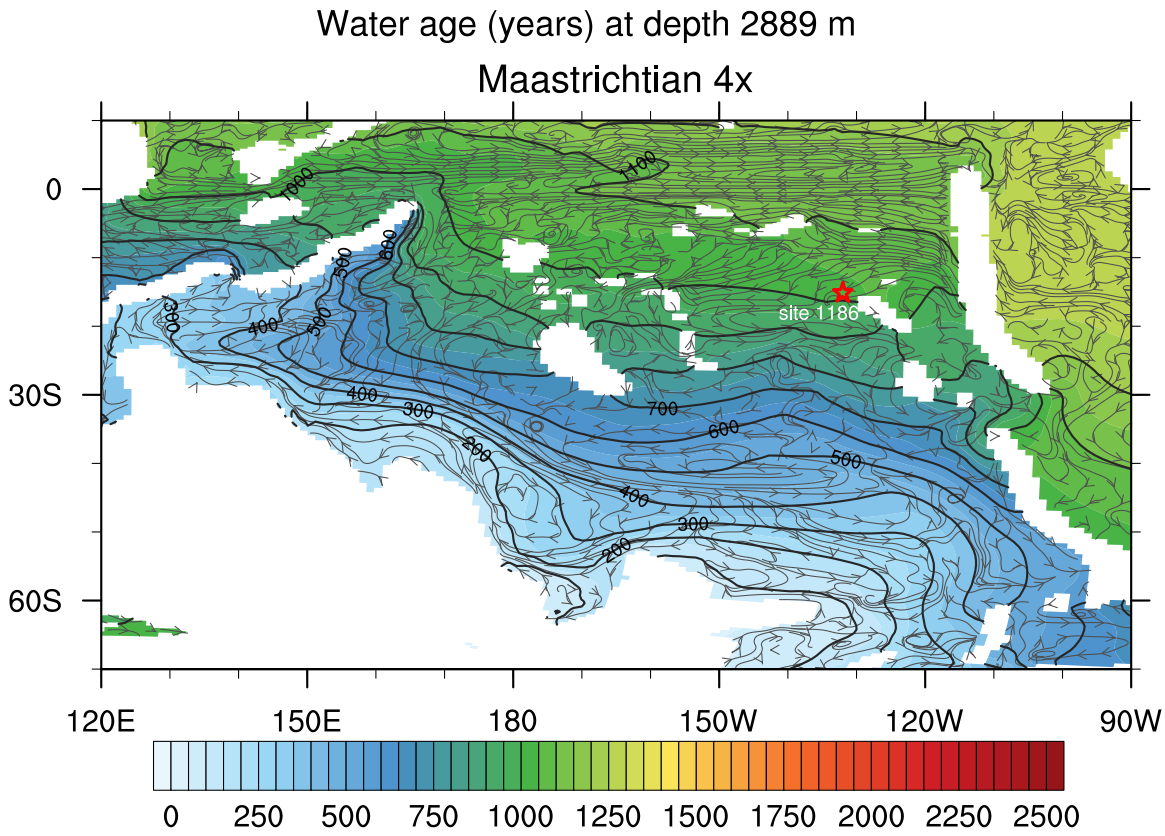

Figure R1. Maastrichtian 4x CO_2 water mass age (100 years black contours) and currents at depth 2900 m in the South Pacific. Estimated paleolocation of site 1186 is shown by the red star.

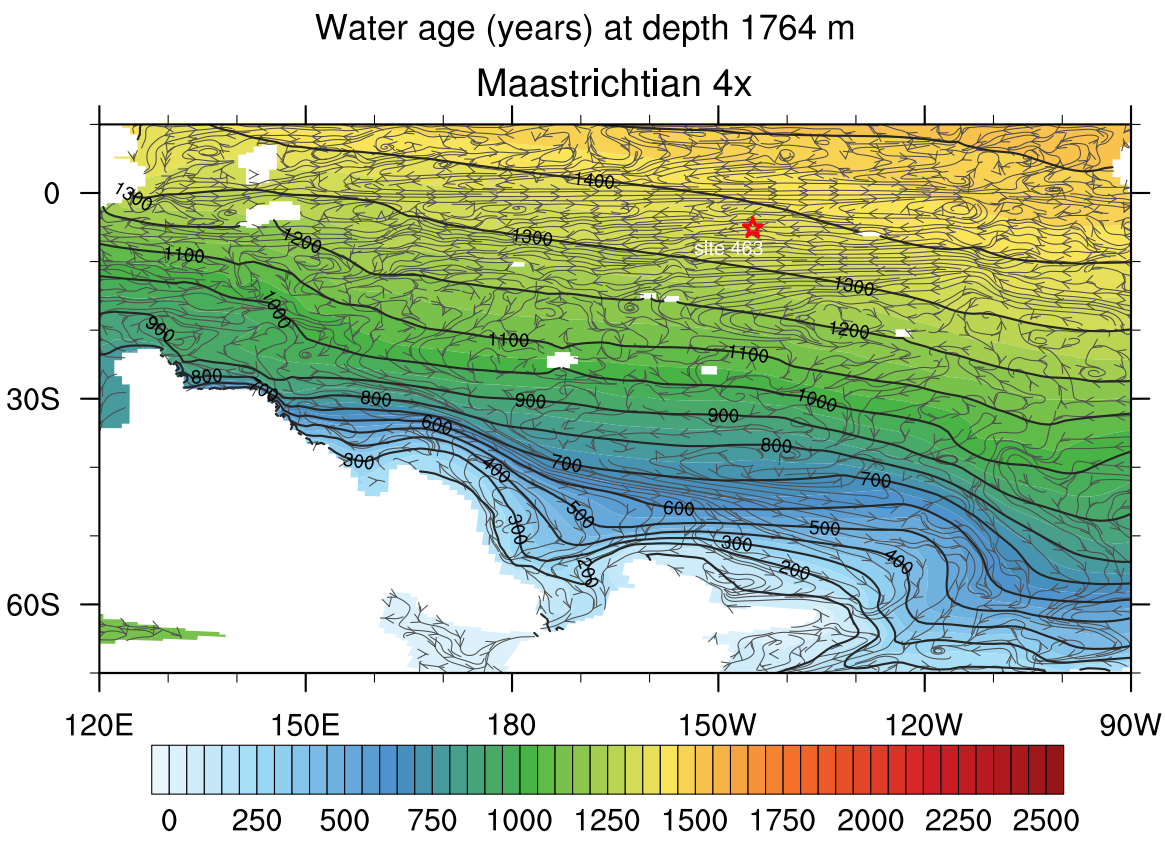

Figure R2. Maastrichtian 4x CO_2 water mass age (100 years black contours) and currents at depth 1700 m in the South Pacific. Estimated paleolocation of site 463 is shown by the red star.

References

Ayache, M., Dutay, J.-C., Arsouze, T., Révillon, S., Beuvier, J., and Jeandel, C.: High-resolution neodymium characterization along the Mediterranean margins and modelling of ε Nd distribution in the Mediterranean basins, Biogeosciences, 13, 2016.

Batenburg, S. J., Voigt, S., Friedrich, O., Osborne, A. H., Bornemann, A., Klein, T., Pérez-Díaz, L., and Frank, M.: Major intensification of Atlantic overturning circulation at the onset of Paleogene greenhouse warmth, Nature communications, 9, 4954, 2018.

Buchs, D. M., Kerr, A. C., Brims, J. C., Zapata-Villada, J. P., Correa-Restrepo, T., and Rodríguez, G.: Evidence for subaerial development of the Caribbean oceanic plateau in the Late Cretaceous and palaeo-environmental implications, Earth and Planetary Science Letters, 499, 62-73, 2018.

Donnadieu, Y., Pucéat, E., Moiroud, M., Guillocheau, F., and Deconinck, J.-F.: A better-ventilated ocean triggered by Late Cretaceous changes in continental configuration, Nature communications, 7, 2016.

Farnsworth, A., Lunt, D. J., O'Brien, C. L., Foster, G. L., Inglis, G. N., Markwick, P., Pancost, R. D., and Robinson, S. A.: Climate Sensitivity on Geological Timescales Controlled by Nonlinear Feedbacks and Ocean Circulation, Geophysical Research Letters, 46, 9880-9889, 2019.

Haynes, S. J., MacLeod, K. G., Ladant, J.-B., Vande Guchte, A., Rostami, M. A., Poulsen, C. J., and Martin, E. E.: Constraining sources and relative flow rates of bottom waters in the Late Cretaceous Pacific Ocean, Geology, 2020.

Hutchinson, D. K., de Boer, A. M., Coxall, H. K., Caballero, R., Nilsson, J., and Baatsen, M.: Climate sensitivity and meridional overturning circulation in the late Eocene using GFDL CM2. 1, Climate of the Past, 14, 2018.

Jeandel, C., Arsouze, T., Lacan, F., Techine, P., and Dutay, J. C.: Isotopic Nd compositions and concentrations of the lithogenic inputs into the ocean: A compilation, with an emphasis on the margins, Chemical Geology, 239, 156-164, 2007.

Lunt, D. J., Valdes, P. J., Jones, T. D., Ridgwell, A., Haywood, A. M., Schmidt, D. N., Marsh, R., and Maslin, M.: CO2-driven ocean circulation changes as an amplifier of Paleocene-Eocene thermal maximum hydrate destabilization, Geology, 38, 875-878, 10.1130/g31184.1, 2010.

Lunt, D. J., Farnsworth, A., Loptson, C., Foster, G. L., Markwick, P., O'Brien, C. L., Pancost, R. D., Robinson, S. A., and Wrobel, N.: Palaeogeographic controls on climate and proxy interpretation, Climate of the Past, 12, 1181-1198, 10.5194/cp-12-1181-2016, 2016.

Moiroud, M., Pucéat, E., Donnadieu, Y., Bayon, G., Guiraud, M., Voigt, S., Deconinck, J.-F., and Monna, F.: Evolution of neodymium isotopic signature of seawater during the Late Cretaceous: Implications for intermediate and deep circulation, Gondwana Research, 36, 503-522, 2016.

Murphy, D. P., and Thomas, D. J.: Cretaceous deep-water formation in the Indian sector of the Southern Ocean, Paleoceanography, 27, PA1211, 10.1029/2011pa002198, 2012.

Murphy, D. P., and Thomas, D. J.: The evolution of Late Cretaceous deep‐ocean circulation in the Atlantic basins: Neodymium isotope evidence from South Atlantic drill sites for tectonic controls,

Geochemistry, Geophysics, Geosystems, 14, 5323-5340, 2013.

Pérez-Díaz, L., and Eagles, G.: South Atlantic paleobathymetry since early Cretaceous, Scientific reports, 7, 1-16, 2017.

Poulsen, C. J., Barron, E. J., Arthur, M. A., and Peterson, W. H.: Response of the Mid-Cretaceous global oceanic circulation to tectonic and CO2 forcings, Paleoceanography, 16, 576-592, 10.1029/2000pa000579, 2001.

Poulsen, C. J., and Zhou, J.: Sensitivity of Arctic climate variability to mean state: insights from the Cretaceous, Journal of climate, 26, 7003-7022, 2013.

Pucéat, E., Lécuyer, C., and Reisberg, L.: Neodymium isotope evolution of NW Tethyan upper ocean waters throughout the Cretaceous, Earth and Planetary Science Letters, 236, 705-720, 2005.

Robinson, S. A., and Vance, D.: Widespread and synchronous change in deep-ocean circulation in the North and South Atlantic during the Late Cretaceous, Paleoceanography, 27, PA1102, 10.1029/2011pa002240, 2012.

Soudry, D., Glenn, C. R., Nathan, Y., Segal, I., and VonderHaar, D.: Evolution of Tethyan phosphogenesis along the northern edges of the Arabian–African shield during the Cretaceous–Eocene as deduced from temporal variations of Ca and Nd isotopes and rates of P accumulation, Earth-Science Reviews, 78, 27-57, 2006.

Tabor, C. R., Poulsen, C. J., Lunt, D. J., Rosenbloom, N. A., Otto-Bliesner, B. L., Markwick, P. J., Brady, E. C., Farnsworth, A., and Feng, R.: The cause of Late Cretaceous cooling: A multimodel-proxy comparison, Geology, 44, 963-966, 10.1130/g38363.1, 2016.

Voigt, S., Jung, C., Friedrich, O., Frank, M., Teschner, C., and Hoffmann, J.: Tectonically restricted deep-ocean circulation at the end of the Cretaceous greenhouse, Earth and Planetary Science Letters, 369, 169-177, 2013.

Winguth, A., Shellito, C., Shields, C., and Winguth, C.: Climate response at the Paleocene–Eocene thermal maximum to greenhouse gas forcing—a model study with CCSM3, Journal of Climate, 23, 2562-2584, 2010.

Zhou, J., Poulsen, C. J., Pollard, D., and White, T. S.: Simulation of modern and middle Cretaceous

marine δ 18O with an ocean‐atmosphere general circulation model, Paleoceanography, 23, 2008.

Zhu, J., Poulsen, C. J., and Tierney, J. E.: Simulation of Eocene extreme warmth and high climate sensitivity through cloud feedbacks, Science advances, 5, eaax1874, 2019.

Zhu, J., Poulsen, C. J., Otto-Bliesner, B. L., Liu, Z., Brady, E. C., and Noone, D. C.: Simulation of early Eocene water isotopes using an Earth system model and its implication for past climate reconstruction, Earth and Planetary Science Letters, 537, 116164, 10.1016/j.epsl.2020.11

Response to comments from Referee #2

This paper presents a set of simulations of the Cenomanian and Maastrichtian, together with selected gateway perturbations, to investigate the intermediate and deep circulation pathways of these time periods and compare with available proxy evidence. There is a substantial amount of work presented here and a thorough examination of all different circulation pathways and possible mechanisms. The text is generally well written and the figures are well composed. This paper is likely suitable for publication in Climate of the Past, subject to revisions.

Thank you for this comment.

My main criticism of the manuscript is that it is very long in describing all details and some of these descriptive parts are less interesting than others. I think the authors ought to prioritise better to focus the manuscript on the most compelling results and conclusions. The text itself is 39 pages, not including references and figures, making it heavy work to read. I have made some suggestions for shortening below; however I encourage the authors to look for their own ways of making it shorter. As a guiding principle, the authors may consider prioritising the two main experiments (Cenomanian vs Maastrichtian), and reducing the discussion of the gateway perturbation experiments.

We acknowledge that the paper is quite long. However, we instead believe that this length is necessary and a strength of the paper because the details of water mass pathways and reorganizations will probably be particularly useful to non-modelers and researchers working with Late Cretaceous ε_{Nd} records. We also note that reviewer #1 requested additional information that we provided. Averaging

reviewer comments does not guarantee successful revisions but the comments from reviewer #1 suggest that our manuscript was not generally considered to be too long.
This said, in the course of the revisions, we have tried to keep your comment in mind by improving readability throughout. We have also tried to establish a clean and intuitive organization with topics divided into clear subsections. Readers with specific interests can read relevant sections and skip portions that are of less interest to them. For instance, as you mention, readers that are not interested in gateway sensitivity experiments can conveniently skip over sections 2. (Paleogeographic considerations), 4.3 (Sensitivity of the Maastrichtian circulation to ocean gateways and atmospheric CO_2) as well as parts of section 5. (Discussion).

One of the main findings of this paper is that Southwest Pacific sinking dominates the deep circulation in all cases. The authors have given some explanation as to why this region always produces sinking (generally low river runoff), but perhaps it is worth mentioning that the Pacific Ocean is the only major basin in these paleogeographies that spans from one polar region to the other (unlike a modern geography where there are two). It is thus virtually guaranteed that equator-to-pole heat transport will drive at least one mode of Pacific sinking that dominates the deep ocean.

You are correct that the Pacific Ocean is the basin that spans from one polar region to the other because the Cenomanian and Maastrichtian North Atlantic Oceans are located at lower latitudes than modern. The Pacific also contains most of the high latitude open ocean area and the majority of the deep ocean area in the Late Cretaceous. Although these considerations render more probable the formation of deep waters in either the North or South Pacific Oceans, there is no requirement for deep water formation on the basis of continental configuration alone. For instance, the 2x CO_2 (560 ppmv) Maastrichtian simulation described in Farnsworth et al. (2019) predicts formation of deep waters in the South Atlantic and Indian Oceans rather than in the North/South Pacific, although Farnsworth et al. (2019) employ the same Maastrichtian paleogeography as we do.

Models and Spinups section
The color scheme used in Figure 1 suffers when in print form: It becomes hard to distinguish between land and shelf – this can easily be fixed by making the land grey. Also, it might be better to use a "cell fill" mode rather than contours, so that the topographic resolution is visible.

Done.

In Figure 2, I'm confused that the model extension runs are only plotted for roughly 300 years each. The methods state (Line 304) that each of these runs has been extended for 950 years. Where is that data?

The first ~ 650 years of the gateway sensitivity experiments have unfortunately not been archived on long-term storage disks and are now lost. However, we would like to point out that this information was and is explicitly stated in the caption of Figure 2 (we have clarified the names of the simulations): "Only the ends of the sensitivity simulations (Deep Labrador Seaway, Deep Drake Passage, Deep Caribbean Seaway and Deep Neotethys Seaway) are shown because the full history of the evolution of these simulations was not conserved."

Results section

I suggest removing Figure 5 and Figure 6, or move them to supplementary, because these figures are visually difficult to digest, require cross-referral back to the captions in Figure 5 and Table 1 to understand properly, and I'm not sure what the story is and why it is interesting. Each of the gateways tends to increase its transport when it is deepened or widened. That is what one would expect. Table 1 already covers all the net transports – to me that is enough.

We agree with you that Table 1 and Figures 5 and 6 are probably redundant. However, we believe that these figures are easier to read in order to get a rapid view of how the intermediate and deep circulations are modified by the opening of specific gateways. It is indeed expected that the deepening of a gateway will lead to an increase in water transport across it. But whether the global pathway of water masses will change in response to the deepening of a gateway is not easily read from Table 1 whereas it is easy to see from Figures 5 and 6. We have thus opted to move Table 1 to the Supplementary Information and to keep Figures 5 and 6 in the main text.

The discussion of the individual gateway perturbation experiments could be substantially shortened. Accordingly, I think parts 3.1 to 3.4 of the Results section could be either reduced or shifted to the supplementary material. Figures 4 and 12 nicely capture the major changes that are seen by altering these gateways. One can see that there is a robust mode of South Pacific sinking in all cases, and there are some modest inter-basin temperature changes resulting from changing certain gateways.

Please refer to your first main comment above.

Discussion section

Section 1 of the Discussion gives a very detailed account of how these simulations agree / do not agree with Donnadieu et al (2016). I find this section unnecessarily long and suggest cutting or shortening it.

The detailed comparison with the results of Donnadieu et al. (2016) was warranted, in our opinion, because this is the only other study (to our knowledge) that actually provides a detailed explanation of deep ocean circulation changes during the Late Cretaceous. Other Late Cretaceous modeling studies mostly focus on surface ocean/climate (Tabor et al. 2016, Lunt et al. 2016, Hunter et al. 2013, Poulsen and Zhou 2013, Niezgodzki et al. 2017, 2019) or skim over deep ocean changes without providing details (Farnsworth et al. 2019). We agree, however, that this section was probably too long and we have therefore shortened it.

The Neodymium discussion is genuinely important, i.e. Sections 2.1 to 2.3 present the available Nd data, and how their earlier and later Cretaceous simulations line up with these data. I would still suggest that some tightening of the text could be made by prioritising the two main experiments (the Cenomanian and Maastrichtian paleogeographies) and reducing the discussion of the individual gateway perturbations.

Please refer to your first main comment above.

Section 2.4 seems like a bit of an afterthought and could be greatly reduced (not nearly as informative as the Nd data comparison). Lines 1014-1016 state, "In summary, the comparison of simulated temperature changes and foraminiferal d18O between the Cenomanian and Maastrichtian does not provide strong evidence for or against proposed changes in ocean circulation patterns or the nature of ocean gateways." That sentiment ought to inspire some reductions to Section 2.4.

Section 2.4 (now section 5.2.4) has been revised following comments from referee #1. We now describe an additional Maastrichtian simulation with prescribed CO_2 levels of 560 ppmv and its comparison with our Cenomanian simulation gives results that fit better with temperature changes inferred from foraminiferal $\delta^{18}O$ between the Cenomanian and the Maastrichtian.

Line / Technical Comments

-L148-149: This sentences changes from past to present tense halfway through, which makes it difficult to read.

Corrected.

-L150-154: Again, the tense changes from past to present in this sentence.

Corrected.

-L192: Antarctica Peninsula: should be Antarctic Peninsula

Corrected.

- L188-213: This paragraph provides a lengthy discussion of past evidence of Drake Passage, without having much bearing on the experimental design. I suggest cutting this. The following paragraph L214-225 explains what changes were made and why and that is much more important.
-L228-250: As above, this paragraph on the Caribbean Seaway doesn't serve a great deal of purpose. The actual experimental design is laid out clearly in the following paragraph.

We thank the reviewer for these suggestions but we believe that the reviews on the tectonic history of the gateways that we modify in the simulations are an important part of the paper. These reviews give insights, albeit sometimes not as constrained as desirable, on the current understanding of the Late Cretaceous configuration of these gateways and provide a complimentary (to proxy records of ε_{Nd}) framework to interpret our results.

-L251: "consistent with these interpretations": This statement is a bit vague. There is a lot of detail in the preceding paragraph, and it's hard to tell which "interpretations" are being referred to here.

Corrected to:
"Our Cenomanian and Maastrichtian paleogeographies are consistent with a shallow Caribbean Seaway."

-L508: "It is also interesting to note that: : :": this is unnecessary word padding.

Removed.

-L543: "decrease supply": grammar.

Corrected.

-L548-550: The words 'slight' or 'slightly' are used 3 times in this sentence, giving the impression that the authors are not convinced about what they are saying here. I suggest removing these.

Thank you. The sentence now reads:

"The water fluxes are generally slightly higher, which is probably linked to the deepening of the North Atlantic and western Neotethyan Oceans winter MLD and associated increase in the vigor of ocean circulation (Fig. S12)."

-L678-679: "each change in gateway profoundly alters the Maastrichtian deep circulation". I'm not convinced by this statement. Some of the key features of the circulation (e.g. MOC) are not greatly affected by these gateway changes.

You are correct that some global features of the ocean circulation, such as the MOC, are only slightly affected. However, the water mass pathways change greatly in most of the gateway sensitivity simulations performed. We have modified the sentence, which now reads:
"With the exception of the Deep Labrador Seaway and the 2x CO_2 experiments, each gateway change profoundly alters Maastrichtian deep ocean water mass pathways."

-L828-835: This sentence is far too long.

The sentence has been cut in two.

-L950: "It is noteworthy that": this is unnecessary word padding.

Removed.

-L958: "concur": I think concur is the wrong word here.

Changed to (l. 1027-1028 of the revised manuscript):
"Thus, we concur with the suggestion that…"

-L1055-1057: Climate of the Past requires authors to provide an online data supplement (unless a compelling reason is given not to). This should be made available to the reviewers before publication.

Done. We have uploaded an online data supplement of model variables on Zenodo:
https://doi.org/10.5281/zenodo.3741722

It is strange that the authors do not use numbered sections for their Level 1 Headings, but from Level 2 and downwards they number the subsections (but without a top-level section number). This leaves the reader somewhat disoriented, since there are multiple instances of Section 1, Section 2, etc

throughout the manuscript. I suggest numbering the top-level headings, re-numbering the lower level sections, and thus complying with the style of Climate of the Past.

Done.

References

Donnadieu, Y., Pucéat, E., Moiroud, M., Guillocheau, F., and Deconinck, J.-F.: A better-ventilated ocean triggered by Late Cretaceous changes in continental configuration, Nature communications, 7, 2016.

Farnsworth, A., Lunt, D. J., O'Brien, C. L., Foster, G. L., Inglis, G. N., Markwick, P., Pancost, R. D., and Robinson, S. A.: Climate Sensitivity on Geological Timescales Controlled by Nonlinear Feedbacks and Ocean Circulation, Geophysical Research Letters, 46, 9880-9889, 2019.

Hunter, S. J., Haywood, A. M., Valdes, P. J., Francis, J. E., & Pound, M. J.: Modelling equable climates of the Late Cretaceous: Can new boundary conditions resolve data–model discrepancies?. Palaeogeography, Palaeoclimatology, Palaeoecology, 392, 41-51, 2013.

Lunt, D. J., Farnsworth, A., Loptson, C., Foster, G. L., Markwick, P., O'Brien, C. L., Pancost, R. D., Robinson, S. A., and Wrobel, N.: Palaeogeographic controls on climate and proxy interpretation, Climate of the Past, 12, 1181-1198, 10.5194/cp-12-1181-2016, 2016.

Niezgodzki, I., Knorr, G., Lohmann, G., Tyszka, J., and Markwick, P. J.: Late Cretaceous climate simulations with different CO2 levels and subarctic gateway configurations: A model‐data comparison, Paleoceanography, 32, 980-998, 2017.

Niezgodzki, I., Tyszka, J., Knorr, G., and Lohmann, G.: Was the Arctic Ocean ice free during the latest Cretaceous? The role of CO2 and gateway configurations, Global and Planetary Change, 177, 201-212, 2019.

Poulsen, C. J., and Zhou, J.: Sensitivity of Arctic climate variability to mean state: insights from the Cretaceous, Journal of climate, 26, 7003-7022, 2013.

Tabor, C. R., Poulsen, C. J., Lunt, D. J., Rosenbloom, N. A., Otto-Bliesner, B. L., Markwick, P. J., Brady, E. C., Farnsworth, A., and Feng, R.: The cause of Late Cretaceous cooling: A multimodel-proxy comparison, Geology, 44, 963-966, 10.1130/g38363.1, 2016.

Revised manuscript with tracked changes

Paleogeographic controls on the evolution of Late Cretaceous ocean circulation

Jean-Baptiste Ladant[1], Christopher J. Poulsen[1], Frédéric Fluteau[2], Clay R. Tabor[3], Kenneth G. MacLeod[4], Ellen E. Martin[5], Shannon J. Haynes[6], Masoud A. Rostami[7]

[1]*Department of Earth and Environmental Sciences, University of Michigan, Ann Arbor, MI, USA*

[2]*Institut de Physique du Globe de Paris, Université de Paris, CNRS, F-75005 Paris, France*

[3]*Department of Geosciences, University of Connecticut, Storrs, CT, USA.*

[4]*Department of Geological Sciences, University of Missouri, Columbia, MO, USA*

[5]*Department of Geosciences, Williamson Hall 362, University of Florida, Gainesville, FL, USA*

[6]*Department of Geosciences, Guyot Hall, Princeton University, Princeton, NJ, USA*

[7]*Ecology, Evolution and Conservation Biology Department, University of Nevada, Reno, NV, USA*

Abstract

Understanding of the role of ocean circulation on climate during the Late Cretaceous is contingent on the ability to reconstruct its modes and evolution. Geochemical proxies used to infer modes of past circulation provide conflicting interpretations for the reorganization of the ocean circulation through the Late Cretaceous. Here, we present climate model simulations of the Cenomanian (100.5 – 93.9 Ma) and Maastrichtian (72.1 – 66.1 Ma) stages of the Cretaceous with the

CCSM4 earth system model. We focus on intermediate (500 – 1500 m) and deep (> 1500 m) ocean circulation, and show that while there is continuous deep-water production in the southwestern Pacific, major circulation changes occur between the Cenomanian and Maastrichtian. Opening of the Atlantic and Southern Ocean, in particular, drives a transition from a mostly zonal circulation to enhanced meridional exchange. Using additional experiments to test the effect of deepening of major ocean gateways in the Maastrichtian, we demonstrate that the geometry of these gateways likely had a considerable impact on ocean circulation. We further compare simulated circulation results with compilations of ε_{Nd} records and show that simulated changes in Late Cretaceous ocean circulation are reasonably consistent with proxy-based inferences. In our simulations, consistency with the geologic history of major ocean gateways and absence of shift in areas of deep-water formation suggest that Late Cretaceous trends in ε_{Nd} values in the Atlantic and southern Indian Oceans were caused by the subsidence of volcanic provinces and opening of the Atlantic and Southern Oceans rather than changes in deep-water formation areas and/or reversal of deep-water fluxes. However, the complexity in interpreting Late Cretaceous ε_{Nd} values underscores the need for new records as well as specific ε_{Nd} modeling to better discriminate between the various plausible theories of ocean circulation change during this period.

1. Introduction

Over the last several decades, a wealth of proxy data established that the Cretaceous period was characterized by a greenhouse climate, with warmer than modern temperatures and an absence of perennial polar ice sheets (e.g., Barron, 1983; Jenkyns et al., 2004; O'Brien et al., 2017). This characterization draws on paleontological and paleobotanical data, including the findings of fossils of ectothermic species (e.g., Tarduno et al., 1998) and woody vegetation (e.g., Bowman et al., 2014) at polar latitudes, as well as geochemical studies indicating warm sea surface and deep ocean temperatures at all latitudes (e.g., Wilson and Norris, 2001; Pucéat et al., 2003; Friedrich et al., 2012; MacLeod et al., 2013; O'Brien et al., 2017; Huber et al., 2018). Successive refinements of the data

indicating Cretaceous warmth also reveal a greater variability within Cretaceous climates than often portrayed and includes carbon cycle perturbations referred to as ocean anoxic events (OAE, e.g., Schlanger and Jenkyns, 1976; Jenkyns, 2010) and intervals of cooler climatic conditions indicated by evidence for polar sea ice (Davies et al., 2009; Bowman et al., 2013) and possibly short-lived polar ice sheets (Price, 1999; Ladant and Donnadieu, 2016). Global paleotemperature compilations confirm this variability and provide evidence of global warming through the Early Cretaceous to early Late Cretaceous (Cenomanian-Turonian) interval of maximum temperatures followed by cooling through the end of the Cretaceous (Cramer et al., 2011; O'Brien et al., 2017; Huber et al., 2018).

Early attempts at modeling past climates with atmosphere-only global climate models suggested that Cretaceous warmth was the result of paleogeographic changes and higher atmospheric CO_2 concentrations (Barron and Washington, 1982, 1984, 1985). The role of paleogeographic changes on global temperature evolution across the Cretaceous has been debated for a long time (Poulsen et al., 2001; Donnadieu et al., 2006; Fluteau et al., 2007). Recent experiments with models of higher complexity and higher resolution support only a weak impact of Cretaceous paleogeographic changes on global temperature evolution (Lunt et al., 2016; Tabor et al., 2016). In contrast, model simulations (Poulsen and Zhou, 2013; Tabor et al., 2016) and paleo-CO_2 reconstructions (Fletcher et al., 2008; Wang et al., 2014) suggest that atmospheric CO_2 concentrations provided a first order control on Late Cretaceous temperatures. Indeed, compilations of paleo-CO_2 concentrations across the Cretaceous suggest that CO_2 and temperatures broadly increased to peak levels during the Cenomanian and Turonian thermal maximum, before decreasing throughout the Late Cretaceous (Wang et al., 2014). The comparison between model simulations and proxy reconstructions of sea surface temperatures (SST) provides further support for a Late Cretaceous cooling trend driven by decreasing CO_2 levels (Tabor et al., 2016).

Late Cretaceous cooling is expressed heterogeneously at a regional scale and reveals inter-basinal variations in both the surface and deep ocean (Friedrich et al., 2012; O'Brien et al., 2017; Huber et al., 2018). For instance, records from the North Atlantic and Indian Ocean show cooling from the Turonian to the mid-Campanian and stabilization or warming afterward, whereas records from the Pacific Ocean and from the Atlantic and Indian sectors of the Southern Ocean show gradual

cooling from the Turonian to the Maastrichtian (e.g., MacLeod et al., 2005; Huber et al., 2018). These distinct regional trends suggest that the pathways followed by water masses and connections between ocean basins changed during the Late Cretaceous as a result of the evolving paleogeography.

This conjecture is corroborated by studies of the temporal trends and spatial variations in the neodymium (Nd) composition of seawater (i.e. the ratio of $^{143}Nd/^{144}Nd$, expressed as ε_{Nd}). Seawater ε_{Nd} values are mainly controlled by export of dissolved Nd through continental weathering and fluvial runoff to the ocean (e.g., Frank, 2002; Goldstein and Hemming, 2003; Tachikawa et al., 2017) but mass-balance calculations have shown that additional sources, such as exchange with continental margins (or Boundary Exchange, Lacan and Jeandel, 2005), are required to close the Nd budget (Tachikawa et al., 2003; Lacan and Jeandel, 2005; Arsouze et al., 2007; Rempfer et al., 2011). Because the residence time of Nd in the ocean is shorter than the oceanic mixing time and initial Nd isotopic ratios are not totally overprinted by particle and/or boundary exchange during circulation (e.g., Frank, 2002; Tachikawa et al., 2003; Rempfer et al., 2011), the ε_{Nd} composition of water masses acts as a quasi-conservative tracer reflecting the geographical provenance and oceanic pathway of water masses (Piepgras and Wasserburg, 1982; Frank, 2002; Goldstein and Hemming, 2003; Moiroud et al., 2016; van de Flierdt et al., 2016), and, as such, is used as a proxy for past ocean circulation.

Records of Nd isotopes illustrate, in particular, a long-term shift toward more unradiogenic (lower) values in the Atlantic basin between the Turonian and the Campanian (e.g., Robinson et al., 2010; MacLeod et al., 2011; Martin et al., 2012; Robinson and Vance, 2012; Moiroud et al., 2016; Batenburg et al., 2018). However, there is no consensus on the specific modes and evolution of ocean circulation across the Late Cretaceous as interpretation is complicated by the lack of Late Cretaceous ε_{Nd} records in key places and times, by the possibility of modification of ε_{Nd} values along flow paths, and by uncertainties in the paleodepth of sites where ε_{Nd} values were documented. Illustrating this lack of consensus, deep-water formation during the Late Cretaceous has been hypothesized to occur (alternatively or concurrently) in most high-latitudes basins, including the South Atlantic and Indian Ocean (e.g., Robinson et al., 2010; Murphy and Thomas, 2012; Robinson and Vance, 2012), North Atlantic (e.g., MacLeod et al., 2011; Martin et al., 2012), North Pacific (e.g., Hague et al., 2012; Thomas et al., 2014; Dameron et al., 2017) and South Pacific (e.g., Thomas et al., 2014; Dameron et

al., 2017; Haynes et al., 2020), as well as possibly in the low latitudes (e.g., Friedrich et al., 2008; MacLeod et al., 2008; MacLeod et al., 2011).

Numerical models have been instrumental in providing a framework for interpreting the paleoceanographic data and in shedding light on new hypotheses, yet the location of possible sources of deep-water differs among simulations almost as much as it does among conclusions of proxy studies (e.g., Brady et al., 1998; Poulsen et al., 2001; Otto-Bliesner et al., 2002; Zhou et al., 2008; Monteiro et al., 2012; Donnadieu et al., 2016; Ladant and Donnadieu, 2016; Lunt et al., 2016). Numerous factors may explain this spread, in particular differences in model complexity and resolution and differences in the paleogeography employed, which may vary across model studies (Donnadieu et al., 2016; Lunt et al., 2016; Tabor et al., 2016). Even within identical Cretaceous time slices, there can be significant differences in paleogeographic reconstructions resulting in additional uncertainty regarding the areas of deep-water formation as well as the configuration of oceanic gateways, and thereby the modes of ocean circulation (e.g., Donnadieu et al., 2016; Lunt et al., 2016; Farnsworth et al., 2019). The considerable impact of breaching a continental barrier or closing an oceanic seaway has long been demonstrated in idealized and paleoclimatic model studies (e.g., Toggweiler and Samuels, 1995; Poulsen et al., 2003; Sijp and England, 2004; Sepulchre et al., 2014; Donnadieu et al., 2016; Elsworth et al., 2017; Ladant et al., 2018; Tabor et al., 2019).

Inter-basinal differences in temperature evolution and shifts in the global ocean circulation therefore point toward a critical role of paleogeographic reorganizations, such as the geometry of oceanic basins or the opening, closure and depth changes of oceanic gateways, regardless of the evolution of atmospheric CO_2 during the Late Cretaceous. To our knowledge, only one coupled ocean-atmosphere model study focused on the evolution of global ocean circulation during the Late Cretaceous (Donnadieu et al., 2016). Using Cenomanian-Turonian and Maastrichtian simulations, Donnadieu et al. (2016) demonstrated a shift toward a more vigorous ocean circulation in the Atlantic between the Cenomanian and the Maastrichtian with an associated shift from deep-water formation in the South Pacific (Cenomanian) to the South Atlantic and Indian Ocean (Maastrichtian). These changes are associated with a reversal of deep-water fluxes across the Caribbean Seaway between North and South America, which provides a possible explanation for decreasing ε_{Nd} values throughout

the Atlantic during the Late Cretaceous (Donnadieu et al., 2016). That study further suggested that paleogeographic evolution during the Late Cretaceous eliminated conditions necessary for the occurrence of OAEs (Donnadieu et al., 2016).

In this contribution, we present a comparison of Cenomanian and Maastrichtian simulations (as well as a number of sensitivity experiments) similar to the Donnadieu et al. (2016) study but using a recent and higher resolution earth system model. We evaluate the effect of changes in the depth of major Maastrichtian gateways including the Labrador Seaway, Drake Passage, Caribbean Seaway and Neotethys Seaway, as well as the effect of decreasing the atmospheric CO_2 concentration. The paper is organized as follows: First, we briefly review the paleogeographic history of major Late Cretaceous gateways to describe the rationale behind prescribed gateway changes. We then explore the evolution of the global ocean circulation in the Late Cretaceous with a particular focus on the changes in intermediate and deep-water currents across the globe. Finally, we compare our simulated ocean circulation with compilations of geochemical data in order to provide an updated picture of the global ocean circulation at the close of the Mesozoic era.

2. Paleogeographic considerations

Advances in the knowledge of the geological history of ocean gateways, combined with modeling of the likely effects of those changes, may provide critical arguments in favor of some modes of Late Cretaceous ocean circulation over others. This section summarizes observations on Late Cretaceous paleogeography in critical regions relative to the Cenomanian (~ 95 Ma) and early Maastrichtian (~ 70 Ma) paleogeographic reconstructions used in our model simulations and sensitivity experiments. These two reconstructions are based on proprietary paleogeographies provided by Getech Plc (Fig. 1), which have been introduced by Lunt et al. (2016) and Tabor et al. (2016).

2.1. Equatorial Atlantic

Rifting between western Africa and eastern Brazil began during the Early Cretaceous (Mascle et al., 1988). Marine waters invaded this narrow corridor from both ends during the Early Aptian and a shallow marine connection between the Central and South Atlantic oceans existed around 104 Ma (Brownfield and Charpentier, 2006; Ye et al., 2017). The NE-SW motion of the South American plate relative to the African plate was accommodated across transform-related marginal ridges dividing the Equatorial Atlantic Ocean into narrow basins during Albian-Cenomanian (Basile et al., 2005; Jones et al., 2007), which restricted seawater exchanges between the Central and South Atlantic oceans and favored euxinic conditions and black shale deposition in these basins (Pletsch et al., 2001; Ye et al., 2017). Deep-water exchange among basins remained limited from the Turonian to the middle Coniacian (Pletsch et al., 2001), but the disappearance of black shales in the Equatorial Atlantic during the Campanian suggests the initiation of a reliable supply of oxygenated deep water from the South Atlantic Ocean at this time (Jones et al., 2007), thereby marking the beginning of a fully opened connection between the Central and South Atlantic oceans.

Our Cenomanian and Maastrichtian paleogeographies (Fig. 1) are consistent with this geological history of the Equatorial Atlantic Seaway. In our Cenomanian paleogeography, this gateway is restricted to a narrow channel with a maximum depth of ~ 2000 m, whereas in the Maastrichtian paleogeography, the Atlantic is opened to full deep-water connection (> 3000 m) between the North and South Atlantic.

2.2. Labrador and East Greenland Seaways

Rifting in the Labrador Sea began during the Early Cretaceous, possibly as early as the Valanginian (Dickie et al., 2011), but the onset of sea-floor spreading took place between the Campanian and the Danian (Roest and Srivastava, 1989; Chalmers and Pulvertaft, 2001). This onset was associated with a deepening of the Labrador Sea as indicated by the presence of agglutinated foraminifera from the Maastrichtian onwards (Kuhnt et al., 1989; Setoyama et al., 2017). East of Greenland, the subsidence of the shallow seas occurred later during the Paleocene (Gernigon et al., 2019).

The proto Labrador Sea is closed in our Cenomanian paleogeography (Fig. 1). Although evidence suggests that a proto Labrador Sea potentially existed before the Campanian (Dickie et al., 2011), it would have been restricted to shallow depths with limited influence on interbasinal exchange due to the absence of a northward connection to the Arctic Ocean. The configuration of the proto Labrador Sea in our Maastrichtian paleogeography (Fig. 1) is in line with the distribution of agglutinated foraminifera (Setoyama et al., 2017), with shallow seas East of Greenland and a deeper proto Labrador Sea to the south. However, the exact paleodepth of the Maastrichtian Labrador and East Greenland seas is still poorly constrained. We investigate the possibility of the existence of deeper marine channels in the Maastrichtian northern North Atlantic by deepening the Labrador and East Greenland seas to 4000 m. This sensitivity experiment represents an end-member of the deepest paleogeographic configuration of the northern North Atlantic in the Maastrichtian and we note that a deep East Greenland Sea is not supported by Cretaceous geologic evidence.

2.3. Drake Passage

The history of Drake Passage is intertwined with the evolution of the South America–Antarctic Peninsula–Scotia plate system (Eagles, 2016). The geometrical arrangement of southern South America and the Antarctic Peninsula (AP) has been a matter of debate since the pioneering work of Wegener (1924). Paleomagnetic inclinations measured in rocks from the Fuegian Andes have been shown to be statistically indistinguishable from those of the Antarctic Peninsula for the Late Cretaceous (Poblete et al., 2016), suggesting that the tip of the AP remained close to Tierra del Fuego. In addition, rocks from the Navarino microplate (Fuegian Andes) recorded a 100° counterclockwise rotation over the last 120 Myr, which suggests that the AP and the southern Andes formed a linear and continuous margin during the Early Cretaceous (Poblete et al., 2016). Likewise, a clockwise rotation was found in the apparent polar wander path of the AP coeval with the rotation of the Navarino microplate, thus confirming the oroclinal bending of the Fuegian Andes (Milanese et al., 2019). During the Cenomanian the oroclinal bending was at an early stage, such that the tip of the South American plate was still connected to the AP, with the possible existence of a land bridge allowing terrestrial and fresh water vertebrate taxa interchange (Poblete et al., 2016). The presence of a land

bridge for terrestrial exchange does not exclude the possible existence of seawater connections, but indicates that any connections would have been restricted to shallow water depths. The oroclinal bending continued during the Late Cretaceous but the AP and southernmost South America remained close to each other during the Maastrichtian. This geography is supported by paleontological evidence placing the onset of terrestrial faunistic isolation in South America in the Late Paleocene around 58 Ma (Reguero et al., 2014). The final disruption of the AP-Patagonia system occurred during the Early Eocene but the development of deep-water exchange through the Drake passage only began during the Late Eocene (Scher and Martin, 2006; Lagabrielle et al., 2009). In summary, although the complexity of the South America–Antarctic Peninsula–Scotia plate system's geologic history still hampers comprehensive tectonic reconstructions of the Drake Passage region during the Late Cretaceous, recent evidence indicates that any potential seawater connection would have been restricted to shallow water.

In our Cenomanian paleogeography, the deepest part of the Drake Passage reaches ~ 800 m along a narrow corridor, while in the Maastrichtian, only upper ocean water exchange is possible through the Drake Passage as its deepest part reaches ~ 400 m. Thus, although our Cenomanian Drake Passage is relatively deep, our Cenomanian and Maastrichtian paleogeographic reconstructions are broadly consistent with paleomagnetic and paleontological data (Fig. 1). However, alternative paleogeographic reconstructions exist, in which the Drake Passage exhibits an even deeper configuration (Sewall et al., 2007; Donnadieu et al., 2016; Niezgodzki et al., 2017). Because the recent study of Donnadieu et al. (2016) documents only minor changes to the global ocean circulation for depths of the Drake Passage lower than 1000 m, we have chosen to prescribe a full deep-ocean connection (4000 m) in our sensitivity experiment in order to maximize the potential impact of the deepening of Drake Passage on ocean circulation, even if these abyssal depths are probably exaggerated for the Maastrichtian (Fig. 1).

2.4. Caribbean Seaway

The Caribbean region has a complex geological evolution, which started during the Jurassic with the dislocation of Pangaea (Pindell and Kennan, 2009). Rifting between North and South

America during the Jurassic and Early Cretaceous led to the opening of the proto-Caribbean Seaway. To the west, subduction of the Farallon plate beneath the proto-Caribbean plate during the Early Cretaceous formed an oceanic volcanic arc stretching from the northwestern tip of South America to the southern tip of North America (Pindell and Kennan, 2009). Emplacement of the Caribbean Large Igneous Province (CLIP) starting in the Cenomanian marked a turning point in the history of the Caribbean region. This large (4 million km^3) basaltic oceanic plateau was formed from 94–89 Ma (Andjić et al., 2019, and references within) or 95–83 Ma (Dürkefälden et al., 2019) from volcanism driven by melting during the initial plume head stage of the Galapagos hotspot. The CLIP was initially located along the southern edge of the North America plate and the northwestern edge of the South America plate, westward of the oceanic island arc (Andjić et al., 2019). Constructed from 8 – 20 km of thick but warm (buoyant) basaltic flows emplaced on the oceanic crust of the Farallon plate, the CLIP prevented subduction of the Caribbean plate (Pindell and Kennan, 2009). During the Cenomanian, the CLIP was located in the Caribbean Seaway and its buoyancy restricted exchange to shallow water passages (Buchs et al., 2018), including local subaerial emergence, as indicated by volcaniclastic deposits exposed in the Western Cordillera of Colombia (Buchs et al., 2018). The CLIP then progressively moved eastward relative to the North and South American plates during the Late Cretaceous and new subduction zones were initiated on both the east and west sides of the CLIP, leading to new volcanic oceanic arcs (Pindell and Kennan, 2009). Paleontological evidence also supports restricted water exchange between the Pacific and the Atlantic during the latest Cretaceous (Iturralde-Vinent, 2006; Ortiz-Jaureguizar and Pascual, 2011). Recent research, therefore, suggests that the Caribbean Seaway was relatively shallow across the Late Cretaceous interval.

Our Cenomanian and Maastrichtian paleogeographies are consistent with a shallow Caribbean Seaway. The Cenomanian Caribbean Seaway is deeper than that of the Maastrichtian, which is in reasonable agreement with the progressive formation of the CLIP and its eastward motion between the North and South American plates (Buchs et al., 2018). Although geologic evidence does not support the existence of a deep-water connection between the Pacific and the Atlantic in the Late Cretaceous, alternative paleogeographic reconstructions have been employed, in which the Caribbean Seaway is opened to deep flow (Sewall et al., 2007; Donnadieu et al., 2016). As we did for the Drake Passage,

we investigate the consequences of prescribing a full deep-ocean connection through the Caribbean Seaway, by deepening the southern portion of this seaway to 4000 m (Fig. 1).

2.5. Neotethys Seaway

The Neotethyan Ocean exhibits a complex geological history. There is evidence for Late Cretaceous marine exchange between the Central Atlantic Ocean and the Neotethyan Ocean, which mostly occurred through narrow and deep corridors (Stampfli, 2000; Stampfli and Borel, 2002; Nouri et al., 2016). These corridors formed during the final break-up of the Pangaea supercontinent, which led to the opening of the Alpine Tethyan Ocean during the Early Jurassic coeval with the opening of the Central Atlantic Ocean (Stampfli and Borel, 2002). The Alpine Tethyan Ocean began to close in the Early Cretaceous in response to the rotations of Africa plate and the Iberian plate (Stampfli and Borel, 2002). During the Late Cretaceous, two deep marine corridors located on both sides of the Anatolides-Taurides permitted water exchanges between the Central Atlantic Ocean and the Neotethyan Ocean (Stampfli and Borel, 2002; Nouri et al., 2016) but it is unclear whether bathymetric sills locally restricted these exchanges to shallow depths (Stampfli and Borel, 2002).

In our paleogeographic reconstructions, the Cenomanian Neotethys allows a deep-water marine connection between the eastern Neotethys and the North Atlantic, whereas the Maastrichtian Neotethyan Ocean does not (Fig. 1). The continued convergence of the African and Eurasian plates throughout the Late Cretaceous (Stampfli and Borel, 2002) can be tentatively used to support the existence of deeper connections in the Cenomanian than the Maastrichtian, but existing uncertainties still preclude any firm conclusions on the absence of deep-water connection through the Neotethyan Ocean in the Maastrichtian. Here, as above, we investigate the consequence of a full deep-ocean connection (4000 m depth) between the Neotethyan Ocean and the North Atlantic.

3. Model description and experimental design

The simulations are performed with the CCSM4 earth system model (Gent et al., 2011, and references therein). Our CCSM4 setup is comprised of the POP2 dynamic ocean model, the CAM4 atmosphere model, the CLM4 land surface model and the CICE4 sea ice model. The atmosphere and land-surface components run on a finite-volume grid at 1.9° x 2.5° resolution with 26 uneven vertical levels, while the ocean and sea-ice components run on a rotated pole distorted grid at roughly 1° resolution with 60 vertical levels that vary in thickness with depth.

We perform two baseline simulations of the Cenomanian and early Maastrichtian, which are branched from the 1500-year long CEN and MAA simulations described in Tabor et al. (2016). The simulations are respectively run for 500 and 850 additional years with prescribed vegetation fields adapted from Sewall et al. (2007) rather than the dynamic vegetation model of Tabor et al. (2016) because the latter produced low vegetation density at high latitudes that did not agree well with fossil-based reconstructions (Tabor et al., 2016). As a result, simulated high latitude land surface temperatures tended to be too cold and seasonally variable. Switching to prescribed vegetation, based on Sewall et al. (2007), helped reduce this temperature bias. Other boundary conditions do not change: the atmospheric CO_2 concentration is set to 1120 ppm (4 times the preindustrial atmospheric levels, PAL = 280 ppm) in line with proxy-based reconstructions (Wang et al., 2014). Other greenhouse gas concentrations are set to their preindustrial values. We use a modern Earth orbital configuration and the total incoming solar irradiance is reduced to appropriate Cenomanian and Maastrichtian values of 1353.9 and 1357.18 $W.m^{-2}$ respectively, following Gough (1981).

The gateway sensitivity experiments, in which either the Labrador Seaway, Drake Passage, Caribbean Seaway, or Neotethys Seaway, is deepened to 4000 m, are branched from the 850-year long extension of our Maastrichtian simulation. Note that we refer to these bathymetric regions as gateways (or seaways) for simplicity although they may not be gateways in its truest sense (i.e. a narrow passage connecting two otherwise separated ocean basins). The baseline Maastrichtian case and four sensitivity experiments are each run for another 950 years. We also perform another sensitivity experiment in which atmospheric CO_2 levels are decreased to 560 ppm (2x PAL) in a Maastrichtian configuration because proxy records indicate that the latest Cretaceous was a time of lower CO_2 concentrations than the Cenomanian (e.g., Breecker et al., 2010; Wang et al., 2014; Foster et al.,

2017). As the Cenomanian and baseline Maastrichtian simulations, the 2x CO_2 simulation is branched from the 1500-year long MAA2x simulation described in Tabor et al. (2016) and is run for 1350 years with the Sewall et al. (2007) prescribed vegetation fields and keeping the other boundary conditions identical to that of the baseline Maastrichtian experiment. In total, the Cenomanian and 2x CO_2 Maastrichtian simulations have been run for 2000 and 2850 years respectively, whereas the baseline Maastrichtian and the gateway sensitivity simulations have been run for 3300 years. Note that the baseline Maastrichtian and 2x CO_2 Maastrichtian simulations are identical to those used in Haynes et al. (2020).

At the end of integration, the simulations have reached quasi-equilibrium in the deep ocean, as characterized by timeseries of temperature and meridional overturning circulation (MOC, Fig. 2). A small residual trend exists in the intermediate ocean of the Maastrichtian simulation (1000 m temperatures), which is probably linked to the interval of MOC intensification in this simulation (Fig. 2). This small trend is unlikely to affect the outcomes of this study because the patterns of the ocean circulation do not change during the interval of lower MOC intensity.

Our version of CCSM4 incorporates an ideal age tracer of water masses, a common tool for tracking water mass pathways. Ideal age is an excellent tracer in a fully equilibrated ocean but for an ocean that is initiated from an unequilibrated state (as in this study), the ideal age tracer is affected by the spinup history and does not track the equilibrium circulation. To use this tracer quantitatively in this study, the simulations would require an additional 2000 years of integration, a computational expense that we could not afford. Alternative techniques, such as Newton-Krylov solvers, exist to estimate the equilibrium values of ocean tracers in an offline procedure (e.g., Bardin et al., 2014; Lindsay, 2017), and such analyses be the focus of future work. In this paper, we use the ideal age tracer only as a qualitative, complementary diagnostic of deep-water formation regions.

Results presented in the following sections are averaged over the last 100 years of each simulation. We first describe general characteristics of the surface climate, the global overturning circulation, and how ocean temperatures respond to changing paleogeography. Next, we focus on the intermediate and deep circulation and analyze how circulation patterns differ between the Cenomanian and the Maastrichtian. To characterize differences, we track the exchange of water across major

oceanic sections by calculating positive and negative water fluxes (Table S1) for three depth ranges—upper ocean (< 500 m depth), intermediate ocean (500 – 1500 m) and deep ocean (> 1500 m). Note that we refer to the net exchange across a section as the sum of positive and negative fluxes across the section. Simulated changes in ocean circulation between the Cenomanian and the Maastrichtian and between the Maastrichtian and the sensitivity experiments are then compared to previous modeling studies and geochemical data.

4. Results

4.1. Cenomanian circulation

4.1.1. Surface climate and global overturning circulation

The global-average annual surface ocean (upper 100 m) temperature of the Cenomanian simulation reaches 26.1 °C. Maximum upper ocean temperatures of more than 34 °C are found in the low-latitudes in the western Pacific Ocean and in the Saharan epicontinental sea in Africa, whereas the eastern Pacific Ocean is much cooler because of wind-driven upwelling (Fig. 3A). Relatively warm (> 10 °C) waters exist in the high-latitudes in the Southern Ocean and the North Pacific, though high-latitude coastal and Arctic Ocean waters are colder. Arctic Ocean mean surface ocean temperatures average 2.7 °C. The cold conditions in the Arctic Ocean allow for the formation of winter sea ice (Fig. S1). The Southern Ocean does not freeze seasonally with the exception of an inlet between the Antarctic and Australian continents (Fig. S1).

The modeled upper ocean salinity generally correlates with patterns of precipitation minus evaporation (PME). The highest open ocean salinities are found in subtropical evaporative areas in the center of major ocean gyres while lower values are found in the equatorial Neotethyan Ocean and western Pacific and in the high-latitudes (Fig. 3B and 3C). The Arctic Ocean contains low salinity values reflecting the fact that it is a nearly enclosed basin in a region of net freshwater input. In addition, freshwater input from continental rivers affects the spatial distribution of salinity (Fig. 3D), in particular in coastal areas and epicontinental seas. The epicontinental northwestern part of Asia is a

region of low salinity due to the isolation of this seaway from the open ocean and of the supply of freshwater from runoff and precipitation. Other low salinity coastal waters are found at equatorial latitudes in enclosed epicontinental basins on the eastern coast of West Africa (Saharan epicontinental sea) and on the northwestern coast of South America as well as in the isolated high-latitude basin located between Australia and Antarctica. In contrast, high salinity waters are found in enclosed subtropical basins, such as on the western coast of South America and on the Asian margin of the Neotethyan Ocean as well as in the Gulf of Mexico (Fig. 3B). These high salinity areas correlate with regions of high temperature, low river freshwater input and largely negative PME (Fig. 3A-D).

The Pacific sector of the Southern Ocean is comparatively warmer and more saline than other high-latitude regions. Cooler and fresher waters in the North Pacific are due to the mixing of North Pacific waters with cold, fresh Arctic waters across the Cenomanian Bering Strait. In the Indo-Atlantic sector of the Southern Ocean, seawater salinities are lower than in the Pacific sector due to the large relative freshwater flux from riverine input into a smaller basin (Table S2). The other major reason for this South Pacific anomaly is a temperature- and salt-advection feedback linked to the winter deepening of the mixed-layer depth (MLD) associated with a large area of deep-water formation (Fig. 3E). The same process occurs in the North Atlantic, albeit at a smaller scale in terms of areal extent and of depth reached by sinking waters (Fig. 3F). Predicted global MOC is essentially fed by sinking South Pacific waters, which drive a strong overturning cell in the Southern Hemisphere, with a maximum of ~ 18 Sv around 40°S and 2000 m, and whose lower limb extends to approximately 40°N at depths of ~ 4000 m (Fig. 4A). In the Northern Hemisphere, the formation of intermediate waters in the North Atlantic leads to a weak Atlantic Meridional Overturning Circulation (Figs. 4A and S2), which reaches up to ~ 1500 – 2000 m around 40°N (Fig. S2).

4.1.2. Intermediate (500 – 1500 m) circulation

The intermediate ocean circulation is fed primarily by two sources: upwelling of deep waters and sinking of upper ocean waters to intermediate depths (Fig. 3E and 3F). North Atlantic intermediate waters are composed of upper waters that sink in the North Atlantic, upwelled deep waters from the Neotethyan Ocean that were advected across the Mediterranean (Table S1, Mediterranean section, and Fig. 5A), and weaker inputs of intermediate waters from the Pacific and

central Atlantic (Table S1, Caribbean and Central Atlantic sections, and Fig. 5A). More than 90% of the intermediate waters advected out of the North Atlantic flow westward across the Caribbean Seaway (Table S1, Caribbean and Central Atlantic sections) while the remaining fraction flows southward through the South Atlantic to the Southern Ocean where it is joined by weak transport of Pacific intermediate waters across Drake Passage (Table S1, South Atlantic and Drake sections, and Fig. 5A). The South Atlantic intermediate waters are then advected eastward trough the Indian Ocean and then northeastward to the eastern Neotethyan Ocean (Figs. S3 and S4). These waters eventually flow into the Pacific by joining an eastern Neotethyan Ocean recirculation of Pacific intermediate waters, forming a narrow, intense eastward current that follows the Australian coast (Fig. S4). In contrast, intermediate waters circulating northwestward toward the western Neotethyan Ocean originate exclusively from Pacific intermediate waters. The Pacific intermediate water system is essentially comprised of a mixture of North Atlantic intermediate waters that flow westward through the Caribbean Seaway, upwelled Pacific deep waters and recirculated Indian Ocean intermediate waters mentioned above.

4.1.3. Deep (> 1500 m) circulation

The southwestern Pacific is the source region for deep waters in our Cenomanian simulation (Fig. 3E). These sinking waters either fill the deep eastern Pacific basin or are advected westward across the Indonesian section, following a strong coastal current around Australia (Figs. 6A and 7). Deep waters crossing the Indonesian section following this westward current mostly recirculates back to the Pacific and mix with the eastern Pacific deep waters to fill the North Pacific basin. Less than 10% of the westward flowing deep waters that have crossed the Indonesian section are advected southward across the East Indian section to the Southern Ocean (Table S1, Indonesian and East Indian sections). Deep waters exported northward toward to western Neotethyan Ocean mostly come from a deep intermediate westward current that follows the southern tip of Asia between ~ 800 and 2400 m (Fig. 7C and Table S1, Indo-Asian and Tethys sections). In the Southern Ocean, deep waters are advected to the South Atlantic but regions of shallow bathymetry (e.g., the Kerguelen Plateau) largely restrict deep-water flow and these waters ultimately well up to shallower depths (Fig. 6A). The fate of deep waters flowing northward from the Neotethyan basin is similar. These waters are advected across

the western Neotethyan Ocean to the North Atlantic, where they are upwelled to shallower depths because the Caribbean Seaway is closed to deep flow (Fig. 6A). An examination of the zonally averaged ideal age values in the Atlantic basin reveals that the deepest-sinking waters in the North Atlantic winter MLD regions reach the deep ocean (Figs. S5 and 3F). These waters are mostly restricted to the North Atlantic; indeed, only a tiny fraction of North Atlantic deep waters is advected southward into the central Atlantic (Table S1).

In summary, the bathymetric restrictions in the Cenomanian Atlantic, western Neotethys and Southern Ocean largely confine deep-water circulation to the Pacific and eastern Neotethyan Ocean. In contrast, a vigorous intermediate circulation marked by a strong circum-equatorial global current exists, although the restricted Central and South Atlantic basins remain mostly stagnant.

4.2. Maastrichtian circulation

4.2.1. Evolution of surface climate and global overturning circulation

The combined changes in paleogeography and solar constant from the Cenomanian to the Maastrichtian lead to a global SST warming of only ~ 0.1 °C, suggesting that changes in paleogeography may cause cooling that compensates for the increasing solar constant (Lunt et al., 2016). Though the global temperature change is minimal, there are substantial regional temperature and salinity changes at the surface in the Maastrichtian compared to the Cenomanian (Tabor et al., 2016). Maastrichtian North Pacific surface ocean waters warm significantly because of the closure of the Arctic connection (Fig. 8A and 9A). As a result, the Arctic Ocean becomes more enclosed, cools and, as a region of net freshwater input, freshens (Fig. 8 A-D and 9A-B). The reduction in the intensity of the circum-equatorial global current (Table S1 and Fig. 9C-D) in the Maastrichtian reduces coastal upwellings of deeper and colder waters on the northern coast of Africa and South America, leading to surface warming of up to a few degrees. The eastern equatorial Pacific warms because of a weaker Walker circulation, which reduces the east-west ocean temperature gradient (Poulsen et al., 1998; Tabor et al., 2016). The PME in the eastern equatorial Pacific increases in the Maastrichtian and leads to lower salinity (Fig. 8B-C and 9B). The opening of the South Atlantic Ocean and Southern Ocean

during the Late Cretaceous created a wider basin, which allows for a large subpolar gyre to form (Fig. 9D). This gyre reduces the advection of warm and saline subtropical waters into the Southern Ocean along the eastern coast of Africa (Fig. 9C and 9D), and the Southern Ocean cools and freshens as a result (Fig. 9A and 9B). In addition, the Ekman pumping associated with the subpolar gyre leads to upwelling of deeper and colder waters to the surface, which contributes to cooling of the South Atlantic and Indian Oceans. In the northern part of the eastern Neotethyan Ocean, the salinity increase (Fig. 9B) is due to changes in the patterns of surface currents, which limits the northward advection of fresher Neotethyan equatorial waters in the Maastrichtian. Finally, cooling in the North Atlantic and warming in the Pacific sector of the Southern Ocean are related to changes in the MOC (Fig. 4B). In contrast to the Cenomanian, the Maastrichtian North Atlantic does not exhibit deep intermediate water formation (Fig. 8E and 8F). This elimination of proto AMOC weakens the advection of warm and saline subtropical waters into the North Atlantic, leading to surface cooling. Conversely, the intensification of South Pacific deep-water formation drives a more expansive global MOC (Fig. 4B) and is associated with surface warming (Fig. 9A) via reinforcement of the temperature- and salt-advection feedback.

4.2.2. Temperature changes in the intermediate and deep ocean

The Cenomanian to Maastrichtian paleogeographic evolution, in particular the widening of the Atlantic Ocean, the northward migration of the Indian and Australian subcontinents, and the varying configuration of major gateways, results in a complete reorganization of intermediate and deep ocean circulation (Table S1 and Figs. 5A-B and 6A-B). This reorganization leads to significant changes in temperatures in the ocean interior in the Maastrichtian relative to the Cenomanian (Fig. 10 and S6). The global temperature change essentially reflects the Pacific signal because of the size of the Pacific basin in both stages (Fig. S3). In the South Pacific Ocean, increased ventilation in the Maastrichtian explains most of the warming signal (Fig. 10B and S6). In the North Pacific, Maastrichtian intermediate water cooling is attributed to restriction to shallow water depths (< 500 m) of flow through the Caribbean Passage, hampering westward advection of North Atlantic waters below the uppermost ocean layers. It is important to note that this restriction is only significant because, in the Cenomanian, North Atlantic intermediate waters are warmer than North Pacific intermediate waters

494 due to deep-water formation occurring in the North Atlantic. In the Maastrichtian, due to the absence
495 of deep-water formation in the North Atlantic, intermediate waters are colder because of reduced
496 ventilation (Fig. 10C and S6) and the geometry and bathymetry of the Caribbean Seaway and of the
497 western Neotethyan Ocean, which isolates the basin from intermediate and deep waters exchange with
498 the Pacific and Neotethyan Oceans.

499 The northward displacement of India and the widening of the Atlantic in the Maastrichtian
500 paleogeography reduce the isolation of the deep South Atlantic, and this basin is invaded by deep flow
501 from the Pacific via the Indian Ocean (Table S1, East Indian and South African sections, and Fig. 6B)
502 leading to lower temperatures (Fig. 10C and S6). Finally, the Neotethyan basin is mostly warmer in
503 the Maastrichtian than it is during the Cenomanian (Fig. 10D). The small deep ocean warming is
504 explained by advection of warmer deep waters formed in the South Pacific. The larger upper
505 intermediate ocean (centered on ~ 500 m depth) warming is explained by differences in the
506 configuration of the western Neotethyan Ocean. In the Cenomanian simulation, Neotethyan upper
507 intermediate waters, formed in the late winter when the MLD deepens (Fig. 3F), are advected toward
508 the North Atlantic because the western Neotethyan Ocean is open to intermediate and deep waters
509 (Fig. S7A). The closure of the western Neotethyan Ocean to intermediate and deep waters in the
510 Maastrichtian simulation hampers this advection, and flow of these waters shifts southward to the
511 eastern Neotethyan Ocean (Fig. S7B). These sinking upper intermediate waters carry a higher
512 temperature and salinity signal into the eastern Neotethyan Ocean, which can be followed on transects
513 across the Neotethyan Ocean (Fig. S7C-F), and are responsible for the warming of this part of the
514 basin in the Maastrichtian.

515 *4.2.3. Evolution of the intermediate (500 – 1500 m) circulation*

516 With the restriction of intermediate and deep flow through the Caribbean Seaway and the
517 western Neotethyan Ocean, the sources of intermediate waters in the North Atlantic Ocean are deep
518 waters advected from the South Atlantic that are upwelled in the North Atlantic (Fig. 5B) and winter
519 downwelling of upper ocean waters in the northern part of the basin (Fig. 8F). North Atlantic
520 intermediate waters return to the Pacific via the South Atlantic and the Indian Ocean (Table S1),
521 following a strong eastward coastal current around the northern tip of Australia (Fig. S8) similar to

that existing in the Cenomanian simulation (Fig. S4). In the eastern Neotethyan Ocean, intermediate waters are primarily composed of intermediate Pacific waters that flow westward across the Indonesian section between 0 and 10°S (Fig. S8), of eastern Neotethyan Ocean deep waters that are upwelled to shallower depths (Table S1, Indo-Asian section and Fig. 6), and of winter upper ocean waters that sink in the northern part of the eastern Neotethys (Fig. S7B). These eastern Neotethyan Ocean intermediate waters flow eastward into the Pacific following a southward current along the eastern Indian margin and mostly join the strong eastward current circulating around Australia (Fig. S8).

4.2.4. Evolution of the deep (> 1500 m) circulation

In the Maastrichtian, as in the Cenomanian, deep waters are formed in the South Pacific, mostly in the western part of the basin, and flow northwestward along the Australian coast (Fig. 11). Along the northern continental slope of the Australian margin, deep waters either cross the Indonesian section eastward or recirculate to fill the Pacific basin (Table S1 and Fig. 11). As in the Cenomanian, deep waters advected across the Indonesian section then either fill the Indian Ocean (Table S1, East Indian section) or journey northward to recirculate toward the Pacific Ocean or the eastern Neotethyan Ocean (Table S1, Indo-Asian section and Fig. 11). Because the connections through the western Neotethyan Ocean are restricted to shallow flow in the Maastrichtian, there is no deep flow across the western Neotethys (Table S1, Tethys and Mediterranean sections, and Fig. 6B). In contrast, the opening of the South Atlantic and Southern Ocean allows stronger deep-water flow from the Indian Ocean into the South Atlantic (Table S1, East Indian, West Indian and South African sections, and Fig. 6B), which is then advected northward to the North Atlantic (Table S1, South and Central Atlantic sections) and progressively upwelled to shallower depths.

In the Maastrichtian simulation, the net deep circulation appears to flow in the opposite direction of the intermediate circulation (Figs. 5B and 6B). The Maastrichtian circulation is also characterized by more intense meridional exchanges (compare Cenomanian and Maastrichtian meridional sections in Table S1, for instance the East Indian, South Atlantic and Central Atlantic sections) whereas the Cenomanian circulation is dominated by zonal flow (Table S1, for instance the Indonesian, Tethys and Caribbean sections).

4.3. Sensitivity of the Maastrichtian circulation to ocean gateways and atmospheric CO_2

As shown above, changes in paleogeography between the Cenomanian and Maastrichtian lead to substantial changes in simulated intermediate and deep ocean circulation. In this section, we analyze the influence of specific gateways and lower atmospheric CO_2 levels on Maastrichtian ocean circulation.

4.3.1. Deepening of the Labrador Seaway

4.3.1.1. Temperature changes in the ocean

Deepening the Labrador Seaway only marginally impacts the global ocean circulation. In this experiment, as in the baseline Maastrichtian configuration, deep-water formation takes place in the South Pacific and mostly in the western part of that basin. The maximum winter MLD in both hemispheres is only weakly different from that of the Maastrichtian (Fig. S9A) and the resulting MOC is nearly identical in structure and intensity (Fig. 4C). In the northern North Atlantic and western Neotethyan Ocean, the slight deepening of the maximum winter mixed layers (Fig. S9A) is associated with surface ocean warming, whereas the surface ocean cools south of Greenland (Fig. 12A). There are only minor temperature changes in other oceanic basins or in the ocean interior (Fig. 12A and S10).

The pattern of upper ocean temperature change is linked to the altered bathymetry of the Deep Labrador Seaway experiment, leading to substantial reorganization of upper ocean currents in the northern North Atlantic (Fig. S11). In the Maastrichtian simulation, waters originating from the North Atlantic subtropical latitudes are largely confined south of Greenland because the shallow bathymetry of the seas bathing the east of Greenland and modern Europe (Fig. S11A). An intense southward flow originating from higher Arctic latitudes exist along the eastern margin of Greenland. This flow then circulates southeastward around the southern edge of the Eurasian continent toward the western Neotethyan Ocean. In the Deep Labrador Seaway experiment, the deepening of the seas south and east of Greenland breaks the confinement of North Atlantic subtropical waters south of Greenland, which

are instead advected eastward toward the western Neotethyan Ocean along the southern margin of the Eurasian continental landmass (Fig. S11B). This eastward current also blocks the southern penetration of the east Greenland current originating from Arctic latitudes, the intensity of which is also reduced. In summary, warm subtropical waters flow eastward in the Deep Labrador Seaway experiment rather than being confined south of Greenland, which cools the upper ocean there and warms the western part of Europe. In the region east of Greenland, the decreased supply of cold high-latitudes waters leads to warming (Fig. 12A).

4.3.1.2. Intermediate and deep circulation changes

There are no changes in the direction of intermediate and deep-water transports across major oceanic sections in the Deep Labrador Seaway experiment relative to the Maastrichtian simulation (Figs. 5B-C and 6B-C). The water fluxes are generally slightly higher, which is probably linked to the deepening of the North Atlantic and western Neotethyan Oceans winter MLD and associated increase in the vigor of ocean circulation (Fig. S12).

4.3.2. Deepening of the Drake Passage

4.3.2.1. Temperature changes in the ocean

Deepening of the Drake Passage has a more significant effect on global ocean circulation than the deepening of the Labrador Seaway. Although deep-water formation still occurs in the South Pacific, the intensity of the MOC decreases (Fig. 4D) because deep-water formation is greatly reduced in the South Pacific, in particular along the eastern edge of Zealandia (Fig. S9B). At the latitudes of the Drake Passage, the MLD increases across the whole South Pacific (Fig. S9B) because of the establishment of a deep-water connection through the Drake Passage, which increases the intensity of the eastward current in the South Pacific. The reduction in the intensity of deep-water formation drives upper ocean temperature cooling in the South Pacific, which is partly carried, albeit weakly, at depth to the Atlantic through the Drake Passage (Figs. 12B and S13). The Atlantic is thus better ventilated because the deep Drake Passage connection allows newly formed, young deep waters to invade the Atlantic (Table S1). In contrast, the North Pacific and Neotethyan Oceans are less well ventilated

because of lower rates of deep-water formation and a lower advection of deep waters across the Indonesian section (Table S1), associated with a small warming.

4.3.2.2. Intermediate circulation changes

The intermediate circulation with an open Drake Passage undergoes only a few changes relative to the Maastrichtian. An eastward current develops across Drake Passage and joins the southward flow from the Atlantic Ocean. This increase in the net supply of intermediate waters in the Southern Ocean (Table S1, Drake, South Atlantic and South African sections) drives a reversal of the intermediate circulation west of India (Table S1, West Indian section, and Figs. 5B and 5D). This northward water flux enhances the intensity of the intermediate circulation in the eastern Neotethyan Ocean (Table S1, Indo-Asian section) but the structure of the circulation does not change (Figs. S8 and S14). The Pacific intermediate circulation is also similar in the Drake Passage experiment as it is in the Maastrichtian simulation.

4.3.2.3. Deep circulation changes

The deep circulation in the equatorial eastern Neotethyan Ocean and at the Neotethyan-Pacific boundary does not change (Fig. S14), but opening the Drake Passage to deep circulation significantly reduces the flux of deep-water flowing westward across the Indonesian section and into the Indian sector of the Southern Ocean (Table S1 and Fig. 6D). This change is balanced by eastward flow across the Drake Passage, which becomes the dominant source of deep waters in the Atlantic sector of the Southern Ocean. In the Indian and Neotethyan Oceans, most of the water flow directions are similar to the Maastrichtian simulation except west of India where the net southward deep-water flow stops. In contrast to the Maastrichtian simulation, with deepening of the Drake Passage, deep waters in the South and North Atlantic mostly originate from Pacific waters flowing eastward through the Drake Passage rather than waters from the Indian Ocean.

4.3.3. Deepening of the Caribbean Seaway

4.3.3.1. Temperature change in the ocean

Similar to the deepening of the Drake Passage, the opening of the Caribbean Seaway to deep flow causes profound restructuring of the global ocean circulation. Deep-water formation continues to

take place in the South Pacific with a reduction in the depth of the winter mixed-layer east of Zealandia relative to the Maastrichtian simulation (Fig. S9C). Consequently, the global MOC is slightly weaker between 2000 and 3000 m (Fig. 4E). The deepening of the Caribbean Seaway leads to cooling of the Atlantic intermediate and deep waters and only minor temperature changes in the Pacific, Indian and Neotethyan Oceans relative to the Maastrichtian, whereas it leads to limited and spatially heterogeneous upper ocean temperature changes (Figs. 12C and S15). As in the Deep Drake Passage experiment relative to the Maastrichtian, the Atlantic Ocean is better ventilated in the Deep Caribbean Seaway experiment than in the Maastrichtian simulation, although intermediate and deep waters invade the Atlantic from the north of the basin rather than from the south.

4.3.3.2. Intermediate circulation changes

As in the Deep Drake Passage experiment, deepening the Caribbean Seaway does not cause major changes to the modeled global intermediate circulation compared to the Maastrichtian simulation. Changes include the development of weak exchanges of similar magnitude between the Atlantic and the Pacific across the Caribbean Seaway as well as the reversal of the intermediate flow across the West Indian section (Table S1 and Fig. 5E). However, the fluxes of water transported by these altered flows are small and the overall structure of the intermediate circulation in the Deep Caribbean Seaway remains similar to that of the Maastrichtian (Table S1 and Fig. 5E).

4.3.3.3. Deep circulation changes

The most salient consequence of the deepening of the Caribbean Seaway on the deep circulation is the reversal of the water fluxes in the Atlantic, from a net northward-dominated flow in the Maastrichtian simulation to a southward-dominated flow in the Deep Caribbean Seaway experiment (Figs. 6B and 6E) due to the invasion of Pacific deep waters into the Atlantic. In the Southern Ocean, the net transport of water shifts from westward-dominated transport to eastward-dominated transport across the South African section (Table S1 and Figs. 6B and 6E). As in other Maastrichtian simulations, deep waters formed in the South Pacific flow across the Indonesian section and are either advected into the Indian sector of the Southern Ocean or recirculated to the Pacific (Figs. 11 and S14). However a stronger eastward deep-water flow exists at the southern tip of the Asian continent because of the entrainment created by the opening of the Caribbean Seaway to deep

circulation (Table S1, Figs. 6E and S14). This strong current and the reversal of the net transport of deep waters between the Atlantic and Indian sectors of the Southern Ocean induce a reversal of the deep flow west of India (Table S1, West Indian section and Fig. 6E). The Southern Ocean is filled with a combination of westward-flowing Indian Ocean deep waters and southward-flowing Atlantic deep waters, which originate from the Pacific and have been advected through the Caribbean Seaway.

4.3.4. Deepening of the Neotethys Seaway

4.3.4.1. Temperature change in the ocean

In the Maastrichtian and sensitivity simulations described so far, the Neotethys Seaway is shallow and inhibits intermediate and deep ocean circulation (Fig. 1). The deepening of the Neotethys Seaway causes a significant reorganization of the circulation. As in the Deep Drake Passage and Deep Caribbean Seaway simulations, deep-water formation occurs in the South Pacific, although the maximum late winter MLD is reduced relative to the Maastrichtian simulation (Fig. S9D), leading to a slight slowdown of the global MOC (Fig. 4F). Changes in ocean temperatures are minor except in the North Atlantic and Neotethyan Oceans at intermediate depth (Figs. 12D and S16). At these depths, the eastern Neotethyan Ocean cools slightly and the western Neotethyan and North Atlantic warm slightly (Figs. 12D and S16). These changes are due to the opening of intermediate and deep connections between the North Atlantic and Neotethyan Oceans. The warmer and saltier sinking winter upper intermediate waters (~ 500 m depth) in the eastern Neotethyan Ocean (Fig. S9D) are advected toward the North Atlantic rather than the Indian Ocean (Fig. S17), which leads to the observed intermediate temperature signal. It is noteworthy that this reorganization of water currents caused by the deepening of the Neotethys Seaway is opposite the reorganization caused by the restriction of the Neotethys Seaway that occurs between the Cenomanian and the Maastrichtian (Figs. S7 and S17).

4.3.4.2. Intermediate circulation changes

In the Deep Neotethys Seaway experiment the directions of the net intermediate transports of water across oceanic sections are also similar to that of the Maastrichtian (Table S1 and Fig. 5B and 5F). The deep western Neotethyan Ocean provides an outlet for North Atlantic intermediate waters across the Mediterranean section, which increases the intermediate water fluxes out of the North

Atlantic (Fig. 5F). However, part of these eastward flowing intermediate waters recirculate to the North Atlantic, both in the uppermost intermediate ocean (~ 500 m), where they join the westward flowing waters that have sunk in winter in the eastern Neotethyan Ocean (Fig. S17), and in the deeper intermediate ocean (Fig. S18). As a consequence, the net intermediate water transport across the Mediterranean section only slightly increases from 0.2 Sv in the Maastrichtian simulation to 0.5 Sv in the Deep Neotethys Seaway experiment (Fig. 5F). The invasion of the Neotethyan Ocean with North Atlantic intermediate waters also reduces the inflow of Pacific intermediate waters in the eastern Neotethyan Ocean (Table S1, Tethys and Indo-Asian sections and Figs. 5F and S18), which leads to the reversal of the intermediate flow across the eastern West Indian section (Table S1 and Fig. 5F). Other net intermediate transports remain in the same direction as in the Maastrichtian simulation.

4.3.4.3. Deep circulation changes

The main circulation difference caused by the deepening of the Neotethys Seaway is a reversal of the deep-water flow direction in the Atlantic basin from northward to southward (Figs. 6B and 6F). In the equatorial Neotethyan Ocean and Neotethyan-Pacific boundary, deep water circulation is similar to that in the Maastrichtian simulation (Fig. S14); however, the deep eastward Pacific return flow is reduced (Fig. 6F and Table S1, Indonesian section). This change is because the deepening of the Neotethys Seaway opens a deep-water pathway for westward flowing deep waters formed in the South Pacific. These South Pacific deep waters divide between a southwestward component, which flows into the Indian sector of the Southern Ocean, and a northwestward component, which flows into the Neotethyan Ocean (Fig. 6F). The northwestward deep-water flow across the Neotethyan Ocean induces a reversal of the deep circulation west of India, from a southward-dominated flow in the Maastrichtian to a northward-dominated flow in the Deep Neotethys Seaway experiment. The Neotethyan deep waters then flow into the Atlantic sector of the Southern Ocean via the North Atlantic, which explains the reversal of deep-water flow in this basin. The Southern Ocean is bathed by a combination of deep waters coming from the southern Indian Ocean route and from the Neotethyan-Atlantic route (Fig. 6F).

4.3.5. Decreasing atmospheric CO_2 concentration

4.3.5.1. Temperature changes in the ocean

Reducing the atmospheric CO_2 concentration only marginally impacts the simulated ocean circulation, even though a ~ 2.5 – 3°C cooling is observed both at the surface and in the ocean interior (Fig. 12E and S19). Deep-water formation occurs in the South Pacific as in the Maastrichtian and gateway sensitivity experiments (Fig. S9E). Maximum late winter MLD increases in the western part of the South Pacific and decreases in the eastern part relative to the Maastrichtian simulation. The global MOC slightly intensifies (Fig. 4G) because the MLD increase occurs in the region where deepest waters are formed (Fig. 8E).

4.3.5.2. Intermediate and deep circulation changes

As in the Deep Labrador Seaway experiment, there are no changes in the direction of the intermediate and deep circulation in the 2x CO_2 experiment compared to the Maastrichtian (Figs. 5B and 5G, and 6B and 6G). The more intense 2x CO_2 MOC drives enhancement of the intermediate and deep fluxes (Table S1) across most oceanic sections but the absence of significant changes in the water mass pathways indicate that the simulated cooling is exclusively due to the radiative effect of the lower atmospheric CO_2 concentration.

5. Discussion

With the exception of the Deep Labrador Seaway and the 2x CO_2 experiments, each gateway change profoundly alters Maastrichtian deep ocean water mass pathways. The deepening of the Drake Passage and Caribbean and Neotethys Seaways opens barriers to deep circulation, leading to changes in the intensity of circulation and pathways of deep-water flow. At intermediate depths, gateway changes affect the origin and intensity of intermediate circulation, but have a lesser effect on the flow pathway within and between basins.

5.1. Comparison to previous model results

5.1.1 Late Cretaceous changes in ocean circulation

To our knowledge only Donnadieu et al. (2016) has investigated changes in ocean circulation from the beginning to the end of the Late Cretaceous. That study uses the FOAM model (Jacob, 1997) to conduct simulations of the Cenomanian/Turonian and Maastrichtian using paleogeographies from Sewall et al. (2007). Donnadieu et al. (2016) (hereafter D16) report that the deep ocean circulation in FOAM is highly sensitive to Late Cretaceous paleogeographic evolution and that these paleogeographic changes are responsible for a shift in the sources of Atlantic deep waters and a reversal of the Atlantic deep-water flow, which provide an explanation for the observed decrease in ε_{Nd} in the Atlantic and Indian Ocean during the Late Cretaceous. Our simulations differ substantially from those of D16 in the paleogeography employed, in particular the configuration of ocean gateways, and in the locations of deep-water formation, which critically affects the simulated pathways of intermediate and deep water masses.

The baseline Cenomanian simulation of D16 shows deep-water formation in the North and South Pacific as well as the South Atlantic. North Atlantic deep waters are sourced from the Pacific and enter the Atlantic through a relatively deep Caribbean Seaway (2000-2500 m), whereas deep waters formed in the South Atlantic are mostly advected toward the eastern Neotethyan Ocean (Figs. 2a and 3c in D16). In our Cenomanian simulation, in which the Caribbean Seaway is closed to deep flow, North and South Atlantic deep waters originate from the Pacific via Neotethyan and Indian routes, respectively (Fig. 6A).

The baseline Maastrichtian simulation of D16 exhibits a shift in deep-water formation from the South Pacific to the South Indian Ocean while deep-water formation in the North Pacific and South Atlantic persists. In those simulations, enhanced South Atlantic deep-water formation drives enhanced northward export of deep waters into the North Atlantic, and these deep waters are advected into the Pacific through a deep Caribbean Seaway (Figs. 2b, 3b and 3d in D16). In our baseline Maastrichtian simulation, the South and North Atlantic are ventilated by deep waters forming in the South Pacific and flowing westward along a pathway through the Indian Ocean but the shallow Caribbean and Neotethys Seaways confine deep-water in the North Atlantic. Interestingly, our Deep Caribbean Seaway experiment, in which the configuration of the Caribbean Seaway is closer to that of the Maastrichtian simulation of D16, predicts a Pacific to Atlantic flow of deep waters across the

Caribbean Seaway (Fig. 6E) whereas D16 experiment predicts the opposite. Contrasts in these model results are directly linked to the different areas of deep-water formation in the Southern Ocean predicted by the two models.

The substantial differences between CESM and FOAM and in the details of the simulations make it difficult to unambiguously explain the substantial changes in the source and circulation of deep waters. In comparison to FOAM, CESM is more complex and has higher spatial resolution. In addition, FOAM and CESM simulations differ in the details of the paleogeographies and initial conditions, which hamper explicit examination of why the two models do not form deep waters in the same locations. However, we speculate that freshwater supply via continental runoff is one mechanism that might lead to these different locations of deep-water formation. In both our Cenomanian and Maastrichtian simulations, the South Pacific is a region of low runoff supply relative to the other sectors of the Southern Ocean (Table S1, Figs. 3D and 8D, and Fig. S20A-B). In addition, the higher elevation and more extensive meridional span of the Rocky Mountains in our reconstructions (Fig. S20C-D) compared to the Sewall et al. (2007) paleogeography used by D16 (Figs. 4 and 5 of Sewall et al., 2007) blocks the advection of moisture across North America (e.g., Maffre et al., 2018), which contributes to decreased surface salinity and prevents deep-water formation in the North Pacific. Finally the lower resolution of FOAM in the atmosphere (7.5° longitude by 4.5° latitude) smooths the Rocky Mountains even more. As a consequence, the moisture flux out of the North Pacific driven by Northern Hemisphere Westerlies may be enhanced in D16, leading to increased North Pacific surface salinity and more favorable conditions for deep-water formation.

5.1.2 Sensitivity of ocean circulation to atmospheric CO_2 levels

Ocean circulation is mostly insensitive to reducing the atmospheric CO_2 concentrations in our Maastrichtian configuration. The intermediate and deep water mass pathways are identical although the intensity of the water fluxes across major oceanic gateways is slightly enhanced in the 2x CO_2 simulation (Haynes et al., 2020). This insensitivity of Late Cretaceous ocean circulation to CO_2 levels is consistent with the results of Donnadieu et al. (2016), which shows that Late Cretaceous simulations performed at 2x, 4x and 8x CO_2 PAL predict similar areas of deep-water formation. In contrast,

Farnsworth et al. (2019) recently reported that reducing atmospheric CO_2 levels from 4x to 2x in a Maastrichtian configuration in the HadCM3BL-M2.1aD earth system model led to a shift in deep-water formation area from the South Pacific Ocean to the South Atlantic and Indian Oceans. This high sensitivity to CO_2 only occurs in the Maastrichtian simulation among all the 12 Cretaceous simulations (one per Cretaceous stage) performed by Farnsworth et al., and occurs again only once (in the Selandian stage, ~ 60.6 Ma) among all their 7 Paleogene simulations. In the other simulations, both the 2x and 4x CO_2 simulations predict similar areas of deep-water formation. The temporal proximity of the Maastrichtian and Selandian stages led Farnsworth et al. (2019) to suggest that the time period close to the Cretaceous/Paleogene boundary might be particularly sensitive to atmospheric CO_2 but it is not clear in this case why their simulation of the Danian stage (~ 63.9 Ma) does not exhibit a similar behavior. As Farnsworth et al. (2019) do not provide a detailed analysis of ocean circulation changes in the Maastrichtian and Selandian stages relative to the others, we can only speculate that these changes might be partly caused by high-latitude smoothing, which is performed on the simulations to ensure model stability and which varies between stages (Lunt et al., 2016; Farnsworth et al., 2019).

More generally, the impact of atmospheric CO_2 levels on ocean circulation has been shown to significantly vary in past greenhouse climate modeling work (Poulsen et al., 2001; Lunt et al., 2010; Poulsen and Zhou, 2013; Donnadieu et al., 2016; Hutchinson et al., 2018; Farnsworth et al., 2019; Zhu et al., 2020). The causes for this large spread in results may be diverse and are difficult to isolate but we hypothesize that the model climate sensitivity to CO_2 and the range of atmospheric CO_2 levels investigated could explain such variability. Winguth et al. (2010) report results of Paleocene-Eocene Thermal Maximum (PETM) simulations using the CCSM3 fully-coupled model (with the CAM3 atmospheric model) and show that ocean circulation and deep-water formation areas remain similar regardless of CO_2, although the intensity of overturning decreases with increasing CO_2. More recently, Zhu et al. (2020) report results of PETM simulations performed at 1x, 3x, 6x and 9x CO_2 PAL using the CESM1.2 ESM (with the CAM5 atmospheric model) and document a shift in deep and intermediate water formation areas between 1x and 3x CO_2 and complete cessation of deep-water formation at 6x and 9x CO_2. The climate sensitivity of CESM1.2 has been shown to be greater than that of CCSM3, and, contrary to CCSM3, to increase with background CO_2 levels (Zhu et al., 2019).

Earth System Models with high climate sensitivity to CO_2 may demonstrate a higher sensitivity of ocean circulation to CO_2 because the climate state in which the radiative forcing of CO_2 leads to a warming sufficient to stop deep-water formation can be expected to occur for smaller changes in atmospheric CO_2 levels.

5.2. Evolution of intermediate and deep-water circulation during the Late Cretaceous

5.2.1. Neodymium isotope compilation

A compilation of Cenomanian and Maastrichtian ε_{Nd} values is shown on Fig. 13 and Tables S3 and S4 (modified from Moiroud et al., 2016). The ε_{Nd} values at each site are averaged between 100 Ma and 90 Ma for the Cenomanian and between 75 Ma and 65 Ma for the Maastrichtian. We perform this temporal averaging because the paleogeographies of the Cenomanian and Maastrichtian are not reconstructed with a temporal resolution higher than a few million years. It is thus not possible to attribute a precise age to our Cenomanian (or Maastrichtian) paleogeography, which could equally appropriately represent a 97 Ma or a 92 Ma paleogeography.

The Cenomanian is characterized by Atlantic and southern Indian Ocean ε_{Nd} values that range mainly between ~ –5 to ~ –6 in the intermediate ocean and ~ –6 to ~ –8 in the deep (Fig. 13). Exceptions to this are the anomalously low ε_{Nd} values recorded in the intermediate western equatorial Atlantic (Demerara Rise, MacLeod et al., 2008; Jiménez Berrocoso et al., 2010; MacLeod et al., 2011; Martin et al., 2012). The tropical Pacific has a high ε_{Nd} signature of ~ –3: however, it is only represented by a single data point at Shatsky Rise (Murphy and Thomas, 2012).

From the Cenomanian to the Maastrichtian, ε_{Nd} values generally decrease by ~ 2 to 3 in the Atlantic and southern Indian Oceans. In the Pacific Ocean, Maastrichtian ε_{Nd} values are ~ –3.5 to –5.5 (Fig. 13). These ε_{Nd} trends have been the focus of numerous hypotheses suggesting the reorganization of ocean circulation through the Late Cretaceous (e.g., Robinson et al., 2010; MacLeod et al., 2011; Martin et al., 2012; Robinson and Vance, 2012; Murphy and Thomas, 2013; Voigt et al., 2013; Donnadieu et al., 2016; Moiroud et al., 2016). It has been suggested that the subsidence of large volcanic provinces, such as Kerguelen Plateau, could have decreased the supply of radiogenic material to the Southern Ocean and could have shifted the signature of Maastrichtian deep water masses

formed in the South Atlantic (Robinson et al., 2010) or southern Indian Ocean (Murphy and Thomas, 2012) to lower values. Similar shifts toward lower ε_{Nd} values in the North Atlantic support hypotheses that suggest that by the Maastrichtian, the central and South Atlantic had deepened enough to allow northward export of deep waters from the Southern Ocean to the North Atlantic (Robinson et al., 2010; Murphy and Thomas, 2012; Robinson and Vance, 2012).

The cessation of Pacific deep-water supply across the Caribbean Seaway in combination with an increased deep-water formation in the Atlantic and Indian sectors of the Southern Ocean has also been proposed to the ε_{Nd} shifts toward lower values (MacLeod et al., 2008; Donnadieu et al., 2016). Alternatively, these shifts could be explained by initiation of deep-water formation in the North Atlantic and invasion of the Southern Ocean by North Atlantic deep waters flowing across the equatorial Atlantic (MacLeod et al., 2005; MacLeod et al., 2011; Martin et al., 2012).

All of these hypotheses explain the similarity in deep-water ε_{Nd} values between the North Atlantic, South Atlantic and Indian Oceans in the Maastrichtian (Fig. 13) by greater communication between the basins (Robinson and Vance, 2012; Murphy and Thomas, 2013; Moiroud et al., 2016). Other records instead suggest that bathymetric barriers of the Rio Grande Rise (RGR) – Walvis Ridge (WR) system in the South Atlantic prevented deep north-south flow between the North Atlantic and the Southern Ocean until the Paleogene (Voigt et al., 2013; Batenburg et al., 2018) although recent work suggest that deep channels existed through the RGR-WR system in the Late Cretaceous (Moiroud et al., 2016; Pérez-Díaz and Eagles, 2017).

The opening of the Atlantic and Southern Ocean nonetheless played a major role in the convergent evolution of ε_{Nd} values in the Late Cretaceous by affecting intermediate and deep flow patterns as well as the residence time of water masses and, hence, local ε_{Nd} inputs such as boundary exchange.

5.2.2. Cenomanian circulation

In contrast to the model simulations of Donnadieu et al. (2016) and the observational hypotheses of Murphy and Thomas (2012, 2013) and Robinson et al. (2010), our Cenomanian simulation indicates deep-water formation in the southwestern Pacific, along the eastern coast of

Australia, rather than in the South Atlantic or southern Indian Ocean (Fig. 3E). However, the deep-water pathway simulated in our Cenomanian simulation, with waters traveling from their Southwestern Pacific source into the southern Indian and South Atlantic Oceans following a strong westward current around the Australian continent, is reasonably consistent with existing ε_{Nd} proxy records. These deep waters would potentially have carried low ε_{Nd} values into the Indian and Atlantic sectors of the Southern Ocean because modern ε_{Nd} values of the margins close to the deep-water formation region in our Cenomanian simulation (eastern coast of Australia and Antarctic coast west of the Ross Sea) are typically between ~ –7 and ~ –20 (Jeandel et al., 2007; Roy et al., 2007). In the South Atlantic and southern Indian Ocean, deep-water ε_{Nd} values may have been modified by the addition of radiogenic contributions from recently active volcanic provinces (e.g., Kerguelen Plateau) that would raise the seawater value. Alternatively, it is possible that bathymetric barriers limited southwestern Pacific deep-water advection to the South Atlantic and southern Indian Ocean sufficiently to allow the ε_{Nd} signature of these deep-water to be overprinted by regional ε_{Nd} supply in the Southern Ocean.

South Atlantic and southern Indian Ocean intermediate and deep sites do show a relatively large range of ε_{Nd} values (between ~ –5 and ~ –10, Fig. 13) and there is a wide range of possible ε_{Nd} sources with very different ε_{Nd} values. The African craton and Brazilian shield in the South Atlantic are unradiogenic (ε_{Nd} values < –10) (Jeandel et al., 2007), as are Antarctic terranes in the Atlantic and Indian sectors of the Southern Ocean (Roy et al., 2007). In contrast, the volcanic provinces of Walvis Ridge and Rio Grande Rise (O'Connor and Duncan, 1990; Murphy and Thomas, 2013; Voigt et al., 2013) and large igneous provinces of the Kerguelen Plateau and Rajmahal traps (Mahoney et al., 1995; Coffin et al., 2002) exhibit more radiogenic values (ε_{Nd} values > –5). Precisely attributing the contribution of each source, including input of southwestern Pacific deep waters, to the South Atlantic and southern Indian Ocean ε_{Nd} values is, therefore, difficult.

Our Cenomanian simulation predicts an inflow of intermediate and deep waters into the North Atlantic from the Tethys and Mediterranean sections (Table S1 and Figs. 5A and 6A). These intermediate and deep waters mostly originate from the equatorial and tropical Pacific via an intense eastward current existing between ~ 800 and 2400 m at the southern tip of Asia, which subsequently

follows the eastern coast of Africa into the Neotethyan Ocean and the North Atlantic (Figs. 14A and 7C). Records from the equatorial Pacific (Murphy and Thomas, 2012) shows moderately high ε_{Nd} values (> –6) from the Cenomanian onwards. In addition, modern compilations of the ε_{Nd} signature of the continental margins in the eastern Mediterranean Sea (Ayache et al., 2016) and on the northeastern coast of Africa (Jeandel et al., 2007) indicate relatively radiogenic ε_{Nd} values (> –6). Inputs of radiogenic intermediate and deep waters from the Pacific into the North Atlantic via this Neotethyan pathway, regardless of whether sediment/water exchange in the Neotethyan Ocean may have contributed to their isotopic composition, provides a possible explanation for the ε_{Nd} signature of the deep North Atlantic (Fig. 13), which has more radiogenic values than the nearby North American and North African continents (Jeandel et al., 2007).

Intermediate and deep-water advection through the Neotethyan Ocean constitutes an alternative possibility to the direct deep-water advection from the Pacific to the North Atlantic through the Caribbean Seaway suggested by Donnadieu et al. (2016), which is problematic given that the Caribbean Seaway was probably closed to intermediate and deep-water flow as early as the Cenomanian (e.g., Buchs et al., 2018). However, other events may also have contributed to raising the ε_{Nd} values of North Atlantic intermediate and deep waters. In particular, volcanism related to the initial emplacement of the CLIP in the Caribbean Seaway during the Cenomanian could have supplied radiogenic material to the North Atlantic without requiring intermediate and deep-water exchange across the Caribbean Seaway or the Neotethyan Ocean. This input would raise the ε_{Nd} values of North Atlantic waters and could account for the high ε_{Nd} values (~ –5) observed in Cenomanian samples at Blake Nose in the intermediate North Atlantic (MacLeod et al., 2008). Another possible explanation for Blake Nose and other intermediate North Atlantic ε_{Nd} values could be a local supply of Pacific surface waters in the North Atlantic following a proto-Gulf Stream (Fig. 14B). The radiogenic surface signal could then have been transported to intermediate waters (Fig. 14C) via intermediate water formation in the North Atlantic (Figs. 3F and S5).

As pointed out in many studies, Demerara Rise and Cape Verde ε_{Nd} signatures stand out relative to other intermediate and deep sites (MacLeod et al., 2008; Jiménez Berrocoso et al., 2010; MacLeod et al., 2011; Martin et al., 2012). As in the simulation of Donnadieu et al. (2016), our

Cenomanian simulation does not produce low latitude intermediate or deep-water formation at Demerara Rise, as has been suggested by previous work (Friedrich et al., 2008; MacLeod et al., 2008; MacLeod et al., 2011; Martin et al., 2012). It does, however, show that Demerara Rise is bathed by a mixture of intermediate waters formed in the North Atlantic and originating from the Neotethyan Ocean, while the deeper Cape Verde site is mostly influenced by deeper waters from the Neotethys (Fig. 14C). It has been suggested that the low ε_{Nd} values at Demerara Rise could be due to boundary exchange with detrital material with extremely unradiogenic signature from the nearby Guyana shield (Donnadieu et al., 2016), possibly in conjunction with very restricted local circulation (Moiroud et al., 2016). Our model results support boundary exchange as an explanation for very low Demerara Rise values but we cannot exclude the possibility that climate models are unable to reproduce low-latitude intermediate or deep-water formation at Demerara Rise because of missing processes or insufficiently detailed local paleogeography. Similarly, our results lead us to follow the suggestion that Cape Verde basin values could be driven by local boundary exchange close to the western African craton (Moiroud et al., 2016). We note that this conclusion is consistent with the results of Tachikawa et al. (1999; 2003), which report more unradiogenic values closer to the African continent at a site located in the high organic flux Mauritanian upwelling region rather than at a site located farther from the coast, which suggests a significant influence of boundary exchange processes in this region (Tachikawa et al., 2003).

5.2.3. Late Cretaceous circulation changes

The opening of the Atlantic and Southern Oceans in our Maastrichtian simulations leads to an increased exchange of intermediate and deep waters between ocean basins (Figs. 5B and 6B), in line with previous model simulations (Donnadieu et al., 2016) and proxy-based evidence (e.g., Robinson et al., 2010; MacLeod et al., 2011; Friedrich et al., 2012; Martin et al., 2012; Robinson and Vance, 2012; Murphy and Thomas, 2013; Huber et al., 2018).

The evolution of the ocean circulation between the Cenomanian and the baseline Maastrichtian, 2x CO_2 Maastrichtian or Deep Labrador Seaway experiments is reasonably consistent with the ε_{Nd} evolution to lower values. Because the 2x CO_2 Maastrichtian and Deep Labrador Seaway

circulations are nearly identical to that of the baseline Maastrichtian experiment, we focus on the baseline Maastrichtian simulation. This simulation estimates higher rates of deep water export from the southwestern Pacific to the Indian and Atlantic sectors of the Southern Ocean than the Cenomanian simulation (Fig. 6A-B). The absence of major changes in the provenance of deep currents between our Cenomanian and Maastrichtian model runs in the southern Indian and South Atlantic Oceans suggests that the main cause of the observed decrease in ε_{Nd} in these basins might have been higher inputs of unradiogenic deep waters into the southern Indian and South Atlantic Oceans driven by higher deep-water export rates and, therefore, less time for reactions with more radiogenic sediments (e.g., Haynes et al., 2020). Alternatively, the observed ε_{Nd} trend might be caused by the progressive subsidence of large igneous provinces, such as the Kerguelen Plateau, which would reduce the supply of radiogenic volcanic material to the Southern Ocean (Murphy and Thomas, 2013). These two hypotheses are not mutually exclusive and are difficult to test. However, we note that the shift toward lower ε_{Nd} values in the Indian and South Atlantic Oceans is predicted by the slightly enhanced intensity of ocean circulation in the 2x CO_2 Maastrichtian simulation relative to the baseline Maastrichtian and is consistent with observational and model-based evidence for lower atmospheric CO_2 during the Maastrichtian (e.g., Wang et al., 2014; Tabor et al., 2016; Foster et al., 2017).

In our baseline Maastrichtian simulation, northward-flowing deep waters from the Southern Ocean dominate the Atlantic and could, therefore, advect low ε_{Nd} values to the North Atlantic and explain the observed ε_{Nd} signature shift in this basin (Figs. 6B and 13). This idea is consistent with previous arguments for the onset of an input of southern water masses into the North Atlantic (Robinson et al., 2010; Robinson and Vance, 2012; Murphy and Thomas, 2013). Indeed, in contrast to the separating role of the RGR-WR system on deep water masses suggested by Voigt et al. (2013) and Batenburg et al. (2018), gaps in the RGR-WR system in our Maastrichtian simulation are deep enough to allow northward flow of deep-water.

Other studies have suggested that intermediate and deep waters could be sourced from high (MacLeod et al., 2011; Martin et al., 2012) or from low (Friedrich et al., 2008; MacLeod et al., 2008; MacLeod et al., 2011) latitude regions in the North Atlantic but deep-water formation there is not supported in our Maastrichtian simulation or in other recent coupled climate model simulations of the

995 Late Cretaceous (Donnadieu et al., 2016; Lunt et al., 2016; Niezgodzki et al., 2017; Farnsworth et al.,
996 2019; Niezgodzki et al., 2019). However, North Atlantic deep-water formation in the Cenozoic has
997 been shown to be sensitive to details of North Atlantic configuration and bathymetry (Stärz et al.,
998 2017; Vahlenkamp et al., 2018; Hutchinson et al., 2019). It is, therefore, possible that existing Late
999 Cretaceous paleogeographic reconstructions are not sufficiently detailed, thereby inhibiting the
1000 modeled onset of North Atlantic deep-water production.

1001 The Deep Caribbean Seaway and Deep Drake Passage simulations produce Pacific
1002 intermediate and deep waters that invade the Atlantic Ocean via northern or southern routes,
1003 respectively (Figs. 5D-E and 6D-E). This increased supply of Pacific waters into the Atlantic would be
1004 expected to increase the ε_{Nd} signature of the Atlantic basin, which is at odds with the observed ε_{Nd}
1005 decrease by ~ 2 to 3 units from the Cenomanian to the Maastrichtian (e.g., Robinson et al., 2010;
1006 MacLeod et al., 2011; Martin et al., 2012; Robinson and Vance, 2012; Murphy and Thomas, 2013;
1007 Moiroud et al., 2016). Our simulations, therefore, argue against the presence of these deep gateways
1008 during the latest Cretaceous, in agreement with recent progress in the understanding of the geological
1009 history of these gateways but in notable contrast to the simulations of Donnadieu et al. (2016).

1010 In the Deep Neotethys simulation as in the baseline Maastrichtian simulation, high volumetric
1011 flow rates of deep waters are exported from the southwestern Pacific to the Indian sector of the
1012 Southern Ocean (Fig. 6F), which, in conjunction with the subsidence of volcanic provinces could
1013 explain the ε_{Nd} decrease in this basin. Because the Neotethyan Ocean is open to intermediate and deep
1014 circulation in this experiment, the deep North Atlantic is filled with westward flowing deep waters
1015 from the Neotethyan Ocean, which then flow southward into the South Atlantic. These deep waters are
1016 composed of a mixture of southwestern Pacific deep waters with low ε_{Nd} values traveling across the
1017 Indian Ocean and of deep waters that have circulated in the tropical and equatorial Pacific Ocean and
1018 had their ε_{Nd} signature shifted toward higher values (e.g., Hague et al., 2012; Thomas et al., 2014;
1019 Haynes et al., 2020), before flowing into the eastern Neotethyan Ocean following the southern tip of
1020 Asia between ~ 2000 and 3000 m (Figs. 15 and S14, Deep Neotethys Indonesian section). The low ε_{Nd}
1021 values observed in the Maastrichtian Atlantic could be consistent with a Deep Neotethys Seaway
1022 scenario if deep waters flowing into the North Atlantic were composed of a greater proportion of

Pacific deep waters that traveled along the Indian Ocean and retained lower ε_{Nd} values than Pacific deep waters that traveled along the southern tip of Asia and acquired higher ε_{Nd} values. However, this hypothesis is less elegant and conceptually more complicated than the invasion of the North Atlantic by deep waters from the Southern Ocean with low ε_{Nd} values into the North Atlantic, as suggested by our baseline Maastrichtian (and Deep Labrador Seaway and 2x CO_2 Maastrichtian) simulation. In addition, the Deep Neotethys hypothesis is not easily reconciled with the geological context of a progressively resorbing Neotethyan Ocean during the Late Cretaceous (Stampfli, 2000).

Our Maastrichtian simulations offer no better solution to the low ε_{Nd} signature of Demerara Rise and Cape Verde records (MacLeod et al., 2008; Jiménez Berrocoso et al., 2010; MacLeod et al., 2011; Martin et al., 2012) than local boundary exchange processes within restricted basins (Donnadieu et al., 2016; Moiroud et al., 2016; Batenburg et al., 2018), at least until the extreme end of the Maastrichtian when a convergence of Demerara Rise and other North Atlantic sites ε_{Nd} values is observed (MacLeod et al., 2011). Likewise, our simulations do not provide a particular solution to the high ε_{Nd} values recorded in Newfoundland basin in the Maastrichtian North Atlantic (Fig. 13). Thus, we concur with the suggestion that local processes involving more radiogenic material might contribute to this signal (Robinson and Vance, 2012), possibly as early as the Cenomanian (Fig. 13).

5.2.4. Oxygen and carbon isotopes

In contrast to the limited impact of specific gateway configurations on ocean temperatures in the Maastrichtian (Fig. 12A-D), regional surface and deep temperature changes of as much as ~ 3°C are simulated between the Cenomanian and the Maastrichtian (Fig. 9A and S6). However, even in basins where these regional temperature changes are consistent with the direction of $\delta^{18}O$ changes between the Cenomanian and the Maastrichtian, they fall short of explaining the amplitude of $\delta^{18}O$ change observed in the proxy records (Huber et al., 2018). For example, the ~ 1 to 1.5 ‰ positive benthic $\delta^{18}O$ trend observed at Blake Nose (Huber et al., 2002; Huber et al., 2018) could in part be explained by the ~ 2°C cooling predicted by our model in the North Atlantic (Fig. 10 and S6) between the Cenomanian and the Maastrichtian, but the parallel positive planktic $\delta^{18}O$ trend is not reproduced in our simulations (Fig. 9A). Similarly, in contrast to proxy observations, our model does not predict

any significant temperature change at Exmouth Plateau in the southern Indian Ocean or in the deep equatorial Pacific (Ando et al., 2013; Falzoni et al., 2016). In the Atlantic sector of the Southern Ocean, our model predicts a small cooling, which is consistent with the $\delta^{18}O$ proxy record in terms of direction of change but not in amplitude (Huber et al., 2018).

As demonstrated in detail by Tabor et al. (2016), accounting for lower Maastrichtian atmospheric CO_2 levels allows better consistency between model results of the Cenomanian and Maastrichtian and observations (Fig. 16). North Atlantic Blake Nose temperature decreases by more than 4°C at ~ 1000 m depth if Maastrichtian CO_2 levels are reduced by a factor of 2 relative to Cenomanian levels, in agreement with the ~ 1 to 1.5 ‰ benthic $\delta^{18}O$ trend. This cooling is paralleled by a ~ 2 to 3 °C surface cooling in agreement with the planktic $\delta^{18}O$ record. With a halving of CO_2, the model also predicts a cooling of ~ 2 to 2.5 °C both at the surface and intermediate depth in the Indian Ocean at Exmouth Plateau and in the deep equatorial Pacific at Shatsky Rise, as well as a more pronounced cooling > 4 °C at the surface and ~ 3 °C in the intermediate and deep ocean in the Atlantic sector of the Southern Ocean (Fig. 16 and Tables S3 and S4). These simulated temperature changes are in better agreement with proxy records (Ando et al., 2013; Falzoni et al., 2016; Huber et al., 2018) than in the absence of CO_2 induced cooling, in particular for benthic records. The amplitude of change in planktic $\delta^{18}O$ between the Cenomanian and Maastrichtian is indeed generally larger than that of the benthic $\delta^{18}O$ (Huber et al., 2018).

Part of the mismatch between simulated temperature changes and $\delta^{18}O$ records may also pertain to the fact that foraminiferal $\delta^{18}O$ is a proxy for temperature and seawater $\delta^{18}O$. Foraminiferal $\delta^{18}O$ values are generally converted to temperatures using the consensus value of –1 ‰ for mean ice-free seawater $\delta^{18}O$ (Shackleton and Kennett, 1975; Pearson, 2012) but regional deviations from the global mean seawater $\delta^{18}O$ can exert a strong control on the conversion of foraminiferal $\delta^{18}O$ values to ocean temperatures, in particular in the upper ocean. The mid-Cretaceous simulations of Zhou et al. (2008) with the GENESIS-MOM coupled model indicate significant surface variability in seawater $\delta^{18}O$ in spite of the absence of a river routing scheme. Because precipitation and runoff are depleted in $\delta^{18}O$ relative to seawater, the upper ocean could exhibit lower seawater $\delta^{18}O$ in regions of high

precipitation and/or high runoff input, with a substantial impact on reconstructed ocean temperatures (Huber et al., 2018).

Alternatively, if significant polar ice sheets developed during the Late Cretaceous, which is unlikely during the Cenomanian based on recent observational and model studies (e.g., MacLeod et al., 2013; Ladant and Donnadieu, 2016) but is more debated for the cooler climates of the Maastrichtian (e.g., Miller et al., 1999; Bowman et al., 2013; Ladant and Donnadieu, 2016; Huber et al., 2018), mean seawater $\delta^{18}O$ may have shifted toward higher values. A positive shift in seawater $\delta^{18}O$ would have reduced the magnitude of seawater cooling required to explain the increasing values in foraminiferal $\delta^{18}O$ through the Maastrichtian. However, latest reviews suggest that, in the absence of direct evidence for ice sheet and synchronicity between indirect evidence, Cretaceous ice sheets might only have existed, if ever, as small ice sheets with limited impact on seawater $\delta^{18}O$ (Huber et al., 2018).

Finally, we note that CO_2-induced cooling may play a role in explaining the Cenomanian to Maastrichtian decrease in vertical $\delta^{13}C$ gradients (Huber et al., 2018) because the temperature dependence of metabolic rates in ocean planktonic communities may have increased surface to deep $\delta^{13}C$ gradient in warmer climates (John et al., 2013), by promoting increased rates of primary productivity, thereby enhancing surface $\delta^{13}C$ values, and/or increased remineralization of organic matter, which would enhance the ^{13}C depletion in the ocean interior.

In summary, the comparison of model results to planktic and benthic $\delta^{18}O$ records confirms that prescribing lower atmospheric CO_2 levels in the Maastrichtian configuration is necessary to reproduce the cooling trend observed in the data. However, the absence of changes in ocean circulation with decreasing CO_2 levels and the limited changes in temperature produced by the deepening of gateways compared to that produced by lower CO_2 levels indicate that changes in both atmospheric CO_2 and paleogeography, likely with a strong influence from the nature of ocean gateways, are needed to reconcile model results and different proxy data into an internally consistent picture of evolving ocean circulation across the Late Cretaceous.

6. Conclusion

Our CCSM4 earth system model simulations of the Cenomanian and Maastrichtian demonstrate significant reorganizations of the deep and intermediate ocean circulation during the Late Cretaceous, which are predominantly controlled by the configuration of major oceanic gateways. Our model predicts continuous deep-water formation in the southwestern Pacific in the Late Cretaceous but show that the Cenomanian to Maastrichtian interval witnessed the transition from an essentially zonal ocean circulation during the Cenomanian to one with increased meridional water exchanges during the Maastrichtian. We show that the simulated ocean circulation compares reasonably well to global ε_{Nd} records and that the Caribbean Seaway and Drake Passage were likely restricted to shallow circulation in the Maastrichtian, in agreement with current paleobathymetric knowledge (e.g., Buchs et al., 2018). In contrast, our simulations cannot discriminate whether deep connections existed across the Neotethyan Ocean on the basis of the comparison with ε_{Nd} records.

We are more confident in interpreting large basin-scale ε_{Nd} trends (such as the Atlantic and Indian Oceans ε_{Nd} decrease between the Cenomanian and Maastrichtian) than local ε_{Nd} values. However, our interpretation of the larger patterns in the ε_{Nd} records is limited by several factors. First, paleogeographic uncertainties require that we average ε_{Nd} values over long time intervals. We are therefore bound to miss higher frequency climatic and oceanic variability, which might explain regional ε_{Nd} signatures. Second, most of the neodymium signatures are between ~ -5 and ~ -10, which are relatively "middle-of-the-road" values that could be explained by a large number of plausible, not mutually exclusive, scenarios. Third, spatial and temporal resolution of the data is low for important intervals; there is a real need for increased Cretaceous ε_{Nd} records in particular from the south(western) Pacific and from the Indian Ocean, regions which are critically under sampled. These issues notwithstanding, direct comparison between ε_{Nd} records and oceanic currents is a step forward to understanding the ocean circulation of the Late Cretaceous, with future advances likely requiring specific modeling of the water mass signature in ε_{Nd} (Arsouze et al., 2007; Sepulchre et al., 2014; Gu et al., 2019).

Ultimately, our work highlights the critical impact of gateway configurations in the Late Cretaceous oceanic evolution. The geologic history of major ocean gateways and the continuous deep-water formation in the South Pacific in our simulations suggest that the Late Cretaceous trend in ε_{Nd} values in the Atlantic and southern Indian Oceans was caused by subsidence of volcanic provinces and opening of the Atlantic and Southern Oceans rather than changes in deep-water formation areas and/or reversal of deep-water fluxes. However, other plausible scenarios consistent with Late Cretaceous ε_{Nd} values remain and new studies combining proxy records, detailed paleogeographic reconstructions and ε_{Nd} modeling will therefore be key to improving our understanding of Late Cretaceous climates.

Data availability

All model outputs and scripts for reproducing this work are archived at the University of Michigan or NCAR Cheyenne supercomputer and Campaign storage space. Model variables used to reproduce the figures shown in the manuscript can be found at https://doi.org/10.5281/zenodo.3741722.

Author contributions

JBL performed model simulations with the help of CJP and CRT and model analyses. FF reviewed the paleogeographic history of ocean gateways. All authors contributed to discussing and interpreting the results and writing the paper.

Competing interests

The authors declare that they have no conflict of interest.

Acknowledgments

We thank Stuart Robinson and an anonymous reviewer for insightful comments that greatly improved the manuscript and Yves Goddéris for efficient editorial handling. We acknowledge high-performance computing support from Cheyenne (*doi:10.5065/D6RX99HX*) provided by NCAR's Computational and Information Systems Laboratory, sponsored by the National Science Foundation. We thank Andrew Vande Guchte for the initial setup of the simulations on the NCAR Cheyenne supercomputer. J.-B. Ladant thanks the Institut de Physique du Globe de Paris for providing working office support. This work was supported by NCAR/CISL allocation UMIC0063 to J.-B. Ladant and C. J. Poulsen, Heising-Simons Foundation Grant #2016-05 to C. J. Poulsen, and U.S. National Science Foundation (OCE-1261562) to K. G. MacLeod, E. E. Martin, and C. J. Poulsen.

References

Andjić, G., Baumgartner, P. O., and Baumgartner-Mora, C.: Collision of the Caribbean Large Igneous Province with the Americas: Earliest evidence from the forearc of Costa Rica, Geological Society of America Bulletin, 2019.

Ando, A., Woodard, S. C., Evans, H. F., Littler, K., Herrmann, S., MacLeod, K. G., Kim, S., Khim, B. K., Robinson, S. A., and Huber, B. T.: An emerging palaeoceanographic 'missing link': multidisciplinary study of rarely recovered parts of deep-sea Santonian–Campanian transition from Shatsky Rise, Journal of the Geological Society, 170, 381-384, 2013.

Arsouze, T., Dutay, J. C., Lacan, F., and Jeandel, C.: Modeling the neodymium isotopic composition with a global ocean circulation model, Chemical Geology, 239, 165-177, 2007.

Ayache, M., Dutay, J.-C., Arsouze, T., Révillon, S., Beuvier, J., and Jeandel, C.: High-resolution neodymium characterization along the Mediterranean margins and modelling of ε Nd distribution in the Mediterranean basins, Biogeosciences, 13, 2016.

Bardin, A., Primeau, F., and Lindsay, K.: An offline implicit solver for simulating prebomb radiocarbon, Ocean Modelling, 73, 45-58, 2014.

Barron, E. J., and Washington, W. M.: Cretaceous climate: a comparison of atmospheric simulations with the geologic record, Palaeogeography, Palaeoclimatology, Palaeoecology, 40, 103-133, 1982.

Barron, E. J.: A warm, equable Cretaceous: the nature of the problem, Earth-Science Reviews, 19, 305-338, 1983.

1191 Barron, E. J., and Washington, W. M.: The role of geographic variables in explaining
1192 paleoclimates: Results from Cretaceous climate model sensitivity studies, Journal of
1193 Geophysical Research: Atmospheres (1984–2012), 89, 1267-1279, 1984.
1194 Barron, E. J., and Washington, W. M.: Warm Cretaceous climates: High atmospheric CO2 as
1195 a plausible mechanism, The Carbon Cycle and Atmospheric CO: Natural Variations Archean
1196 to Present, 546-553, 1985.
1197 Basile, C., Mascle, J., and Guiraud, R.: Phanerozoic geological evolution of the Equatorial
1198 Atlantic domain, Journal of African Earth Sciences, 43, 275-282, 2005.
1199 Batenburg, S. J., Voigt, S., Friedrich, O., Osborne, A. H., Bornemann, A., Klein, T., Pérez-
1200 Díaz, L., and Frank, M.: Major intensification of Atlantic overturning circulation at the onset
1201 of Paleogene greenhouse warmth, Nature communications, 9, 4954, 2018.
1202 Bowman, V. C., Francis, J. E., and Riding, J. B.: Late Cretaceous winter sea ice in
1203 Antarctica?, Geology, 41, 1227-1230, 10.1130/g34891.1, 2013.
1204 Bowman, V. C., Francis, J. E., Askin, R. A., Riding, J. B., and Swindles, G. T.: Latest
1205 Cretaceous–earliest Paleogene vegetation and climate change at the high southern latitudes:
1206 palynological evidence from Seymour Island, Antarctic Peninsula, Palaeogeography,
1207 Palaeoclimatology, Palaeoecology, 408, 26-47, 10.1016/j.palaeo.2014.04.018, 2014.
1208 Brady, E. C., DeConto, R. M., and Thompson, S. L.: Deep water formation and poleward
1209 ocean heat transport in the warm climate extreme of the Cretaceous (80 Ma), Geophysical
1210 Research Letters, 25, 4205-4208, 1998.
1211 Breecker, D. O., Sharp, Z. D., and McFadden, L. D.: Atmospheric CO2 concentrations during
1212 ancient greenhouse climates were similar to those predicted for A.D. 2100, Proceedings of the
1213 National Academy of Sciences of the United States of America, 107, 576-580,
1214 10.1073/pnas.0902323106, 2010.
1215 Brownfield, M. E., and Charpentier, R. R.: Geology and total petroleum systems of the Gulf
1216 of Guinea Province of West Africa, US Geological Survey, 2006.
1217 Buchs, D. M., Kerr, A. C., Brims, J. C., Zapata-Villada, J. P., Correa-Restrepo, T., and
1218 Rodríguez, G.: Evidence for subaerial development of the Caribbean oceanic plateau in the
1219 Late Cretaceous and palaeo-environmental implications, Earth and Planetary Science Letters,
1220 499, 62-73, 2018.
1221 Chalmers, J. A., and Pulvertaft, T. C. R.: Development of the continental margins of the
1222 Labrador Sea: a review, Geological Society, London, Special Publications, 187, 77-105,
1223 2001.
1224 Coffin, M. F., Pringle, M. S., Duncan, R. A., Gladczenko, T. P., Storey, M., Müller, R. D.,
1225 and Gahagan, L. A.: Kerguelen hotspot magma output since 130 Ma, Journal of Petrology,
1226 43, 1121-1137, 2002.
1227 Cramer, B. S., Miller, K. G., Barrett, P. J., and Wright, J. D.: Late Cretaceous–Neogene
1228 trends in deep ocean temperature and continental ice volume: Reconciling records of benthic
1229 foraminiferal geochemistry (δ18O and Mg/Ca) with sea level history, Journal of Geophysical
1230 Research, 116, 10.1029/2011jc007255, 2011.
1231 Dameron, S. N., Leckie, R. M., Clark, K., MacLeod, K. G., Thomas, D. J., and Lees, J. A.:
1232 Extinction, dissolution, and possible ocean acidification prior to the Cretaceous/Paleogene
1233 (K/Pg) boundary in the tropical Pacific, Palaeogeography, palaeoclimatology, palaeoecology,
1234 485, 433-454, 2017.
1235 Davies, A., Kemp, A. E., and Pike, J.: Late Cretaceous seasonal ocean variability from the
1236 Arctic, Nature, 460, 254-258, 10.1038/nature08141, 2009.
1237 Dickie, K., Keen, C. E., Williams, G. L., and Dehler, S. A.: Tectonostratigraphic evolution of
1238 the Labrador margin, Atlantic Canada, Marine and Petroleum Geology, 28, 1663-1675, 2011.

Donnadieu, Y., Pierrehumbert, R., Jacob, R., and Fluteau, F.: Modelling the primary control of paleogeography on Cretaceous climate, Earth and Planetary Science Letters, 248, 426-437, 10.1016/j.epsl.2006.06.007, 2006.
Donnadieu, Y., Pucéat, E., Moiroud, M., Guillocheau, F., and Deconinck, J.-F.: A better-ventilated ocean triggered by Late Cretaceous changes in continental configuration, Nature communications, 7, 2016.
Dürkefälden, A., Hoernle, K., Hauff, F., Wartho, J.-A., van den Bogaard, P., and Werner, R.: Age and geochemistry of the Beata Ridge: Primary formation during the main phase (~ 89 Ma) of the Caribbean Large Igneous Province, Lithos, 328, 69-87, 2019.
Eagles, G.: Tectonic reconstructions of the Southernmost Andes and the Scotia Sea during the opening of the Drake Passage, in: Geodynamic evolution of the southernmost Andes, Springer, 75-108, 2016.
Elsworth, G., Galbraith, E., Halverson, G., and Yang, S.: Enhanced weathering and CO2 drawdown caused by latest Eocene strengthening of the Atlantic meridional overturning circulation, Nature Geoscience, 10, 213-216, 2017.
Falzoni, F., Petrizzo, M. R., Clarke, L. J., MacLeod, K. G., and Jenkyns, H. C.: Long-term Late Cretaceous oxygen-and carbon-isotope trends and planktonic foraminiferal turnover: A new record from the southern midlatitudes, Bulletin, 128, 1725-1735, 2016.
Farnsworth, A., Lunt, D. J., O'Brien, C. L., Foster, G. L., Inglis, G. N., Markwick, P., Pancost, R. D., and Robinson, S. A.: Climate Sensitivity on Geological Timescales Controlled by Nonlinear Feedbacks and Ocean Circulation, Geophysical Research Letters, 46, 9880-9889, 2019.
Fletcher, B. J., Brentnall, S. J., Anderson, C. W., Berner, R. A., and Beerling, D. J.: Atmospheric carbon dioxide linked with Mesozoic and early Cenozoic climate change, Nature Geoscience, 1, 43-48, 10.1038/ngeo.2007.29, 2008.
Fluteau, F., Ramstein, G., Besse, J., Guiraud, R., and Masse, J. P.: Impacts of palaeogeography and sea level changes on Mid-Cretaceous climate, Palaeogeography, Palaeoclimatology, Palaeoecology, 247, 357-381, 2007.
Foster, G. L., Royer, D. L., and Lunt, D. J.: Future climate forcing potentially without precedent in the last 420 million years, Nature communications, 8, 14845, 2017.
Frank, M.: Radiogenic isotopes: tracers of past ocean circulation and erosional input, Reviews of geophysics, 40, 1-1-1-38, 2002.
Friedrich, O., Erbacher, J., Moriya, K., Wilson, P. A., and Kuhnert, H.: Warm saline intermediate waters in the Cretaceous tropical Atlantic Ocean, Nature Geoscience, 1, 453, 2008.
Friedrich, O., Norris, R. D., and Erbacher, J.: Evolution of middle to Late Cretaceous oceans--A 55 m.y. record of Earth's temperature and carbon cycle, Geology, 40, 107-110, 10.1130/g32701.1, 2012.
Gent, P. R., Danabasoglu, G., Donner, L. J., Holland, M. M., Hunke, E. C., Jayne, S. R., Lawrence, D. M., Neale, R. B., Rasch, P. J., and Vertenstein, M.: The community climate system model version 4, Journal of Climate, 24, 4973-4991, 2011.
Gernigon, L., Franke, D., Geoffroy, L., Schiffer, C., Foulger, G. R., and Stoker, M.: Crustal fragmentation, magmatism, and the diachronous opening of the Norwegian-Greenland Sea, Earth-Science Reviews, 2019.
Goldstein, S. L., and Hemming, S. R.: Long-lived isotopic tracers in oceanography, paleoceanography, and ice-sheet dynamics, Treatise on geochemistry, 6, 625, 2003.
Gough, D. O.: Solar interior structure and luminosity variations, in: Physics of Solar Variations, Springer, 21-34, 1981.

Gu, S., Liu, Z., Jahn, A., Rempfer, J., Zhang, J., and Joos, F.: Modeling Neodymium Isotopes in the Ocean Component of the Community Earth System Model (CESM1), Journal of Advances in Modeling Earth Systems, 11, 624-640, 2019.
Hague, A. M., Thomas, D. J., Huber, M., Korty, R., Woodard, S. C., and Jones, L. B.: Convection of North Pacific deep water during the early Cenozoic, Geology, 40, 527-530, 10.1130/g32886.1, 2012.
Haynes, S. J., MacLeod, K. G., Ladant, J.-B., Vande Guchte, A., Rostami, M. A., Poulsen, C. J., and Martin, E. E.: Constraining sources and relative flow rates of bottom waters in the Late Cretaceous Pacific Ocean, Geology, 2020.
Huber, B. T., Norris, R. D., and MacLeod, K. G.: Deep-sea paleotemperature record of extreme warmth during the Cretaceous, Geology, 30, 123, 10.1130/0091-7613(2002)030<0123:dsproe>2.0.co;2, 2002.
Huber, B. T., MacLeod, K. G., Watkins, D. K., and Coffin, M. F.: The rise and fall of the Cretaceous Hot Greenhouse climate, Global and Planetary Change, 167, 1-23, 10.1016/j.gloplacha.2018.04.004, 2018.
Hutchinson, D. K., de Boer, A. M., Coxall, H. K., Caballero, R., Nilsson, J., and Baatsen, M.: Climate sensitivity and meridional overturning circulation in the late Eocene using GFDL CM2. 1, Climate of the Past, 14, 2018.
Hutchinson, D. K., Coxall, H. K., O′Regan, M., Nilsson, J., Caballero, R., and de Boer, A. M.: Arctic closure as a trigger for Atlantic overturning at the Eocene-Oligocene Transition, Nature communications, 10, 1-9, 2019.
Iturralde-Vinent, M. A.: Meso-Cenozoic Caribbean paleogeography: implications for the historical biogeography of the region, International Geology Review, 48, 791-827, 2006.
Jacob, R.: Low Frequency Variability in a Simulated Atmosphere Ocean System, PhD, University of Wisconsin-Madison, Madison, Wisconsin, USA., 1997.
Jeandel, C., Arsouze, T., Lacan, F., Techine, P., and Dutay, J. C.: Isotopic Nd compositions and concentrations of the lithogenic inputs into the ocean: A compilation, with an emphasis on the margins, Chemical Geology, 239, 156-164, 2007.
Jenkyns, H. C., Forster, A., Schouten, S., and Damsté, J. S. S.: High temperatures in the late Cretaceous Arctic Ocean, Nature, 432, 888-892, 2004.
Jenkyns, H. C.: Geochemistry of oceanic anoxic events, Geochemistry, Geophysics, Geosystems, 11, Q03004, 10.1029/2009gc002788, 2010.
Jiménez Berrocoso, Á., MacLeod, K. G., Martin, E. E., Bourbon, E., Londoño, C. I., and Basak, C.: Nutrient trap for Late Cretaceous organic-rich black shales in the tropical North Atlantic, Geology, 38, 1111-1114, 2010.
John, E. H., Pearson, P. N., Coxall, H. K., Birch, H., Wade, B. S., and Foster, G. L.: Warm ocean processes and carbon cycling in the Eocene, Phil. Trans. R. Soc. A, 371, 20130099, 2013.
Jones, E. J. W., Bigg, G. R., Handoh, I. C., and Spathopoulos, F.: Distribution of deep-sea black shales of Cretaceous age in the eastern Equatorial Atlantic from seismic profiling, Palaeogeography, Palaeoclimatology, Palaeoecology, 248, 233-246, 2007.
Kuhnt, W., Kaminski, M. A., and Moullade, M.: Late Cretaceous deep-water agglutinated foraminiferal assemblages from the North Atlantic and its marginal seas, Geologische Rundschau, 78, 1121-1140, 1989.
Lacan, F., and Jeandel, C.: Neodymium isotopes as a new tool for quantifying exchange fluxes at the continent–ocean interface, Earth and Planetary Science Letters, 232, 245-257, 2005.
Ladant, J. B., and Donnadieu, Y.: Palaeogeographic regulation of glacial events during the Cretaceous supergreenhouse, Nature communications, 7, 12771, 10.1038/ncomms12771, 2016.

Ladant, J. B., Donnadieu, Y., Bopp, L., Lear, C. H., and Wilson, P. A.: Meridional contrasts in productivity changes driven by the opening of Drake Passage, Paleoceanography and Paleoclimatology, 33, 302-317, 2018.
Lagabrielle, Y., Goddéris, Y., Donnadieu, Y., Malavieille, J., and Suarez, M.: The tectonic history of Drake Passage and its possible impacts on global climate, Earth and Planetary Science Letters, 279, 197-211, 10.1016/j.epsl.2008.12.037, 2009.
Lindsay, K.: A newton–krylov solver for fast spin-up of online ocean tracers, Ocean Modelling, 109, 33-43, 2017.
Lunt, D. J., Valdes, P. J., Jones, T. D., Ridgwell, A., Haywood, A. M., Schmidt, D. N., Marsh, R., and Maslin, M.: CO2-driven ocean circulation changes as an amplifier of Paleocene-Eocene thermal maximum hydrate destabilization, Geology, 38, 875-878, 10.1130/g31184.1, 2010.
Lunt, D. J., Farnsworth, A., Loptson, C., Foster, G. L., Markwick, P., O'Brien, C. L., Pancost, R. D., Robinson, S. A., and Wrobel, N.: Palaeogeographic controls on climate and proxy interpretation, Climate of the Past, 12, 1181-1198, 10.5194/cp-12-1181-2016, 2016.
MacLeod, K. G., Huber, B. T., and Isaza-Londoño, C.: North Atlantic warming during global cooling at the end of the Cretaceous, Geology, 33, 437-440, 2005.
MacLeod, K. G., Martin, E. E., and Blair, S. W.: Nd isotopic excursion across Cretaceous ocean anoxic event 2 (Cenomanian-Turonian) in the tropical North Atlantic, Geology, 36, 811-814, 2008.
MacLeod, K. G., Londoño, C. I., Martin, E. E., Berrocoso, Á. J., and Basak, C.: Changes in North Atlantic circulation at the end of the Cretaceous greenhouse interval, Nature Geoscience, 4, 779, 2011.
MacLeod, K. G., Huber, B. T., Berrocoso, A. J., and Wendler, I.: A stable and hot Turonian without glacial d18O excursions is indicated by exquisitely preserved Tanzanian foraminifera, Geology, 41, 1083-1086, 10.1130/g34510.1, 2013.
Maffre, P., Ladant, J.-B., Donnadieu, Y., Sepulchre, P., and Goddéris, Y.: The influence of orography on modern ocean circulation, Climate dynamics, 50, 1277-1289, 2018.
Mahoney, J. J., Jones, W. B., Frey, F. A., Salters, V. J. M., Pyle, D. G., and Davies, H. L.: Geochemical characteristics of lavas from Broken Ridge, the Naturaliste Plateau and southernmost Kerguelen Plateau: Cretaceous plateau volcanism in the southeast Indian Ocean, Chemical Geology, 120, 315-345, 1995.
Martin, E. E., MacLeod, K. G., Berrocoso, A. J., and Bourbon, E.: Water mass circulation on Demerara Rise during the Late Cretaceous based on Nd isotopes, Earth and Planetary Science Letters, 327, 111-120, 2012.
Mascle, J., Blarez, E., and Marinho, M.: The shallow structures of the Guinea and Ivory Coast-Ghana transform margins: their bearing on the Equatorial Atlantic Mesozoic evolution, Tectonophysics, 155, 193-209, 1988.
Milanese, F., Rapalini, A., Slotznick, S. P., Tobin, T. S., Kirschvink, J., and Olivero, E.: Late Cretaceous paleogeography of the Antarctic Peninsula: New paleomagnetic pole from the James Ross Basin, Journal of South American Earth Sciences, 91, 131-143, 2019.
Miller, K. G., Barrera, E., Olsson, R. K., Sugarman, P. J., and Savin, S. M.: Does ice drive early Maastrichtian eustasy?, Geology, 27, 783-786, 1999.
Moiroud, M., Pucéat, E., Donnadieu, Y., Bayon, G., Guiraud, M., Voigt, S., Deconinck, J.-F., and Monna, F.: Evolution of neodymium isotopic signature of seawater during the Late Cretaceous: Implications for intermediate and deep circulation, Gondwana Research, 36, 503-522, 2016.
Monteiro, F. M., Pancost, R. D., Ridgwell, A., and Donnadieu, Y.: Nutrients as the dominant control on the spread of anoxia and euxinia across the Cenomanian‐Turonian oceanic anoxic event (OAE2): Model‐data comparison, Paleoceanography, 27, 2012.

Murphy, D. P., and Thomas, D. J.: Cretaceous deep-water formation in the Indian sector of the Southern Ocean, Paleoceanography, 27, PA1211, 10.1029/2011pa002198, 2012.
Murphy, D. P., and Thomas, D. J.: The evolution of Late Cretaceous deep‐ocean circulation in the Atlantic basins: Neodymium isotope evidence from South Atlantic drill sites for tectonic controls, Geochemistry, Geophysics, Geosystems, 14, 5323-5340, 2013.
Niezgodzki, I., Knorr, G., Lohmann, G., Tyszka, J., and Markwick, P. J.: Late Cretaceous climate simulations with different CO2 levels and subarctic gateway configurations: A model‐data comparison, Paleoceanography, 32, 980-998, 2017.
Niezgodzki, I., Tyszka, J., Knorr, G., and Lohmann, G.: Was the Arctic Ocean ice free during the latest Cretaceous? The role of CO2 and gateway configurations, Global and Planetary Change, 177, 201-212, 2019.
Nouri, F., Azizi, H., Golonka, J., Asahara, Y., Orihashi, Y., Yamamoto, K., Tsuboi, M., and Anma, R.: Age and petrogenesis of Na-rich felsic rocks in western Iran: Evidence for closure of the southern branch of the Neo-Tethys in the Late Cretaceous, Tectonophysics, 671, 151-172, 2016.
O'Brien, C. L., Robinson, S. A., Pancost, R. D., Sinninghe Damsté, J. S., Schouten, S., Lunt, D. J., Alsenz, H., Bornemann, A., Bottini, C., Brassell, S. C., Farnsworth, A., Forster, A., Huber, B. T., Inglis, G. N., Jenkyns, H. C., Linnert, C., Littler, K., Markwick, P., McAnena, A., Mutterlose, J., Naafs, B. D. A., Püttmann, W., Sluijs, A., van Helmond, N. A. G. M., Vellekoop, J., Wagner, T., and Wrobel, N. E.: Cretaceous sea-surface temperature evolution: Constraints from TEX 86 and planktonic foraminiferal oxygen isotopes, Earth-Science Reviews, 172, 224-247, 10.1016/j.earscirev.2017.07.012, 2017.
O'Connor, J. M., and Duncan, R. A.: Evolution of the Walvis Ridge‐Rio Grande Rise hot spot system: Implications for African and South American plate motions over plumes, Journal of Geophysical Research: Solid Earth, 95, 17475-17502, 1990.
Ortiz-Jaureguizar, E., and Pascual, R.: The tectonic setting of the Caribbean region and the K/T turnover of the South American land-mammal fauna, Boletín Geológico y Minero, 122, 333-344, 2011.
Otto-Bliesner, B. L., Brady, E. C., and Shields, C.: Late Cretaceous ocean: Coupled simulations with the National Center for Atmospheric Research Climate System Model, Journal of Geophysical Research, 107, 10.1029/2001jd000821, 2002.
Pearson, P. N.: Oxygen isotopes in foraminifera: Overview and historical review, The Paleontological Society Papers, 18, 1-38, 2012.
Pérez-Díaz, L., and Eagles, G.: South Atlantic paleobathymetry since early Cretaceous, Scientific reports, 7, 1-16, 2017.
Piepgras, D. J., and Wasserburg, G. J.: Isotopic composition of neodymium in waters from the Drake Passage, Science, 217, 207-214, 1982.
Pindell, J. L., and Kennan, L.: Tectonic evolution of the Gulf of Mexico, Caribbean and northern South America in the mantle reference frame: an update, Geological Society, London, Special Publications, 328, 1-55, 2009.
Pletsch, T., Erbacher, J., Holbourn, A. E. L., Kuhnt, W., Moullade, M., Oboh-Ikuenobede, F. E., Söding, E., and Wagner, T.: Cretaceous separation of Africa and South America: the view from the West African margin (ODP Leg 159), Journal of South American Earth Sciences, 14, 147-174, 2001.
Poblete, F., Roperch, P., Arriagada, C., Ruffet, G., de Arellano, C. R., Hervé, F., and Poujol, M.: Late Cretaceous–early Eocene counterclockwise rotation of the Fueguian Andes and evolution of the Patagonia–Antarctic Peninsula system, Tectonophysics, 668, 15-34, 2016.
Poulsen, C. J., Seidov, D., Barron, E. J., and Peterson, W. H.: The impact of paleogeographic evolution on the surface oceanic circulation and the marine environment within the Mid‐Cretaceous tethys, Paleoceanography, 13, 546-559, 1998.

Poulsen, C. J., Barron, E. J., Arthur, M. A., and Peterson, W. H.: Response of the Mid-Cretaceous global oceanic circulation to tectonic and CO2 forcings, Paleoceanography, 16, 576-592, 10.1029/2000pa000579, 2001.
Poulsen, C. J., Gendaszek, A. S., and Jacob, R. L.: Did the rifting of the Atlantic Ocean cause the Cretaceous thermal maximum?, Geology, 31, 115-118, 10.1130/0091-7613(2003)031, 2003.
Poulsen, C. J., and Zhou, J.: Sensitivity of Arctic climate variability to mean state: insights from the Cretaceous, Journal of climate, 26, 7003-7022, 2013.
Price, G. D.: The evidence and implications of polar ice during the Mesozoic, Earth-Science Reviews, 48, 183-210, 1999.
Pucéat, E., Lécuyer, C., Sheppard, S. M. F., Dromart, G., Reboulet, S., and Grandjean, P.: Thermal evolution of Cretaceous Tethyan marine waters inferred from oxygen isotope composition of fish tooth enamels, Paleoceanography, 18, 1029, 10.1029/2002pa000823, 2003.
Reguero, M. A., Gelfo, J. N., López, G. M., Bond, M., Abello, A., Santillana, S. N., and Marenssi, S. A.: Final Gondwana breakup: the Paleogene South American native ungulates and the demise of the South America–Antarctica land connection, Global and Planetary change, 123, 400-413, 2014.
Rempfer, J., Stocker, T. F., Joos, F., Dutay, J.-C., and Siddall, M.: Modelling Nd-isotopes with a coarse resolution ocean circulation model: Sensitivities to model parameters and source/sink distributions, Geochimica et Cosmochimica Acta, 75, 5927-5950, 2011.
Robinson, S. A., Murphy, D. P., Vance, D., and Thomas, D. J.: Formation of "Southern Component Water" in the Late Cretaceous: Evidence from Nd-isotopes, Geology, 38, 871-874, 10.1130/g31165.1, 2010.
Robinson, S. A., and Vance, D.: Widespread and synchronous change in deep-ocean circulation in the North and South Atlantic during the Late Cretaceous, Paleoceanography, 27, PA1102, 10.1029/2011pa002240, 2012.
Roest, W. R., and Srivastava, S. P.: Sea-floor spreading in the Labrador Sea: A new reconstruction, Geology, 17, 1000-1003, 1989.
Roy, M., van de Flierdt, T., Hemming, S. R., and Goldstein, S. L.: 40Ar/39Ar ages of hornblende grains and bulk Sm/Nd isotopes of circum-Antarctic glacio-marine sediments: implications for sediment provenance in the southern ocean, Chemical Geology, 244, 507-519, 2007.
Scher, H., and Martin, E.: Timing and climatic consequences of the opening of Drake Passage, Science, 312, 428-430, 10.1126/science.1120044, 2006.
Schlanger, S. O., and Jenkyns, H. C.: Cretaceous oceanic anoxic events: causes and consequences, Geologie en mijnbouw, 55, 1976.
Sepulchre, P., Arsouze, T., Donnadieu, Y., Dutay, J. C., Jaramillo, C., Le Bras, J., Martin, E., Montes, C., and Waite, A. J.: Consequences of shoaling of the Central American Seaway determined from modeling Nd isotopes, Paleoceanography, 29, 176-189, 10.1002/2013pa002501, 2014.
Setoyama, E., Kaminski, M. A., and Tyszka, J.: Late Cretaceous–Paleogene foraminiferal morphogroups as palaeoenvironmental tracers of the rifted Labrador margin, northern proto-Atlantic, Grzybowski Foundation Special Publication, 22, 179-220, 2017.
Sewall, J. O., Van De Wal, R. S. W., Van Der Zwan, K., Van Oosterhout, C., Dijkstra, H. A., and Scotese, C. R.: Climate model boundary conditions for four Cretaceous time slices, Climate of the Past, 3, 647-657, 2007.
Shackleton, N., and Kennett, J.: Paleotemperature history of the Cenozoic and the initiation of Antarctic glaciation: oxygen and carbon isotope analyses in DSDP Sites 277, 279, and 281, Initial reports of the deep sea drilling project, 29, 743-755, 1975.

Sijp, W. P., and England, M. H.: Effect of the Drake Passage throughflow on global climate, Journal of physical oceanography, 34, 1254-1266, 10.1175/1520-0485(2004)034, 2004.
Stampfli, G. M.: Tethyan oceans, Geological society, london, special publications, 173, 1-23, 2000.
Stampfli, G. M., and Borel, G. D.: A plate tectonic model for the Paleozoic and Mesozoic constrained by dynamic plate boundaries and restored synthetic oceanic isochrons, Earth and Planetary Science Letters, 196, 17-33, 2002.
Stärz, M., Jokat, W., Knorr, G., and Lohmann, G.: Threshold in North Atlantic-Arctic Ocean circulation controlled by the subsidence of the Greenland-Scotland Ridge, Nature communications, 8, 15681, 2017.
Tabor, C. R., Poulsen, C. J., Lunt, D. J., Rosenbloom, N. A., Otto-Bliesner, B. L., Markwick, P. J., Brady, E. C., Farnsworth, A., and Feng, R.: The cause of Late Cretaceous cooling: A multimodel-proxy comparison, Geology, 44, 963-966, 10.1130/g38363.1, 2016.
Tabor, C. R., Feng, R., and Otto‐Bliesner, B. L.: Climate responses to the splitting of a supercontinent: Implications for the breakup of Pangea, Geophysical Research Letters, 2019.
Tachikawa, K., Jeandel, C., and Roy-Barman, M.: A new approach to the Nd residence time in the ocean: the role of atmospheric inputs, Earth and Planetary Science Letters, 170, 433-446, 1999.
Tachikawa, K., Athias, V., and Jeandel, C.: Neodymium budget in the modern ocean and paleo-oceanographic implications, Journal of Geophysical Research, 108, 10.1029/1999jc000285, 2003.
Tachikawa, K., Arsouze, T., Bayon, G., Bory, A., Colin, C., Dutay, J.-C., Frank, N., Giraud, X., Gourlan, A. T., and Jeandel, C.: The large-scale evolution of neodymium isotopic composition in the global modern and Holocene ocean revealed from seawater and archive data, Chemical Geology, 457, 131-148, 2017.
Tarduno, J. A., Brinkman, D. B., Renne, P. R., Cottrell, R. D., Scher, H., and Castillo, P.: Evidence for extreme climatic warmth from Late Cretaceous Arctic vertebrates, Science, 282, 2241-2243, 1998.
Thomas, D. J., Korty, R., Huber, M., Schubert, J. A., and Haines, B.: Nd isotopic structure of the Pacific Ocean 70–30 Ma and numerical evidence for vigorous ocean circulation and ocean heat transport in a greenhouse world, Paleoceanography, 29, 454-469, 2014.
Toggweiler, J., and Samuels, B.: Effect of Drake Passage on the global thermohaline circulation, Deep Sea Research Part I: Oceanographic Research Papers, 42, 477-500, 1995.
Vahlenkamp, M., Niezgodzki, I., De Vleeschouwer, D., Lohmann, G., Bickert, T., and Pälike, H.: Ocean and climate response to North Atlantic seaway changes at the onset of long-term Eocene cooling, Earth and Planetary Science Letters, 498, 185-195, 2018.
van de Flierdt, T., Griffiths, A. M., Lambelet, M., Little, S. H., Stichel, T., and Wilson, D. J.: Neodymium in the oceans: a global database, a regional comparison and implications for palaeoceanographic research, Philosophical Transactions of the Royal Society A: Mathematical, Physical and Engineering Sciences, 374, 20150293, 2016.
Voigt, S., Jung, C., Friedrich, O., Frank, M., Teschner, C., and Hoffmann, J.: Tectonically restricted deep-ocean circulation at the end of the Cretaceous greenhouse, Earth and Planetary Science Letters, 369, 169-177, 2013.
Wang, Y., Huang, C., Sun, B., Quan, C., Wu, J., and Lin, Z.: Paleo-CO2 variation trends and the Cretaceous greenhouse climate, Earth-Science Reviews, 129, 136-147, 10.1016/j.earscirev.2013.11.001, 2014.
Wilson, P. A., and Norris, R. D.: Warm tropical ocean surface and global anoxia during the mid-Cretaceous period, Nature, 412, 425-429, 2001.

Winguth, A., Shellito, C., Shields, C., and Winguth, C.: Climate response at the Paleocene–Eocene thermal maximum to greenhouse gas forcing—a model study with CCSM3, Journal of Climate, 23, 2562-2584, 2010.
Ye, J., Chardon, D., Rouby, D., Guillocheau, F., Dall'asta, M., Ferry, J.-N., and Broucke, O.: Paleogeographic and structural evolution of northwestern Africa and its Atlantic margins since the early Mesozoic, Geosphere, 13, 1254-1284, 2017.
Zhou, J., Poulsen, C. J., Pollard, D., and White, T. S.: Simulation of modern and middle Cretaceous marine δ18O with an ocean‐atmosphere general circulation model, Paleoceanography, 23, 2008.
Zhu, J., Poulsen, C. J., and Tierney, J. E.: Simulation of Eocene extreme warmth and high climate sensitivity through cloud feedbacks, Science advances, 5, eaax1874, 2019.
Zhu, J., Poulsen, C. J., Otto-Bliesner, B. L., Liu, Z., Brady, E. C., and Noone, D. C.: Simulation of early Eocene water isotopes using an Earth system model and its implication for past climate reconstruction, Earth and Planetary Science Letters, 537, 116164, 10.1016/j.epsl.2020.116164, 2020.

Figure legends

Figure 1. Bathymetry of the Cenomanian and Maastrichtian configurations and enlargements of regions where bathymetric changes were made in the gateway sensitivity experiments.

Figure 2. (A) Timeseries of temperature at the sea surface and in the intermediate (1000 m) and deep (3000 m) ocean, showing that the model has reached quasi-equilibrium at the end of the simulations. The gap between years 850 and 930 in the Maastrichtian simulation (red line) is due to unfortunate loss of data. Only the ends of the sensitivity simulations (Deep Labrador Seaway, Deep Drake Passage, Deep Caribbean Seaway and Deep Neotethys Seaway) are shown because the full history of the evolution of these simulations was not conserved. Note that the first 1500 years of the simulations, described in Tabor et al. (2016), are omitted on this figure. (B) Timeseries of the meridional overturning circulation. Note that the maximum overturning intensity is negative because the circulation is anticlockwise.

Figure 3. Climate diagnostics for the Cenomanian simulation. (A) Surface ocean (upper 100 m) temperature (°C), (B) Surface ocean (upper 100 m) salinity (PSU), (C) Precipitation minus evaporation (mm/day), (D) Runoff freshwater flux (mSv), (E and F) Late winter maximum mixed layer depth (m).

Figure 4. Global meridional overturning circulation (clockwise positive) for each experiment. (A) Cenomanian, (B) Maastrichtian, (C) Deep Labrador Seaway, (D) Deep Drake Passage, (E) Deep Caribbean Seaway, (F) Deep Neotethys Seaway, (G) 2x CO_2 Maastrichtian.

Figure 5. Intermediate (500 – 1500 m) water flow across major oceanic sections defined in Table S1 and represented in green for each simulation. Because flows vary across the range of depth depicted, summed flow in both directions across each section is shown with the larger flux in red and the smaller in orange. Thus, the direction of the red arrow gives the direction of the net intermediate flow across a section and the magnitude of the net flow is given by the difference between the fluxes represented by the red and orange arrows. Abbreviated sections: C (Caribbean), CA (Central Atlantic), D (Drake), EI (East Indian), IA (Indo-Asian), Ind (Indonesian), Med (Mediterranean), SA (South Atlantic), SAf (South African), SC (South China), Tet (Tethys), WI (West Indian).

Figure 6. Deep (> 1500 m) water flow across major oceanic sections defined in Table S1 and represented in green for each simulation. As in Figure 5, because flows vary across the range of depth depicted, summed flow in both directions across each section is shown with the larger flux in red and the smaller in orange. Thus, the direction of the red arrow gives the direction of the net intermediate flow across a section and the magnitude of the net flow is given by the difference between the fluxes represented by the red and orange arrows. Abbreviated sections: C (Caribbean), CA (Central Atlantic), D (Drake), EI (East Indian), IA (Indo-Asian), Ind (Indonesian), Med (Mediterranean), SA (South Atlantic), SAf (South African), SC (South China), Tet (Tethys), WI (West Indian).

Figure 7. Cenomanian deep circulation (3000 m) in (A) the eastern Neotethyan Ocean and (B) the southwestern Pacific Ocean. Orange arrows represent major deep current systems in the eastern Neotethyan Ocean and southwestern Pacific Ocean. Purple contours represent regions of deep waters formation (contour 500 m). Section A-B defines the Indonesian section of Table S1. (C) Fluxes of water across the Indonesian section over the whole water column.

Figure 8. Climate diagnostics for the Maastrichtian simulation. (A) Surface ocean (upper 100 m) temperature (°C), (B) Surface ocean (upper 100 m) salinity (PSU), (C) Precipitation minus evaporation (mm/day), (D) Runoff freshwater flux (mSv), (E and F) Late winter maximal mixed layer depth (m).

Figure 9. Climate diagnostics for the Maastrichtian simulation relative to the Cenomanian simulation. (A) Surface ocean (upper 100 m) temperature difference (°C), (B) Surface ocean (upper 100 m) salinity difference (°C), (C and D) Cenomanian and Maastrichtian barotropic streamfunction (Sv).

Figure 10. Zonally averaged temperature difference (°C) between the Maastrichtian and the Cenomanian simulations. (A) Global average, (B, C, D) Pacific, Atlantic and Indo-Neotethyan average, based on basins defined in Fig. S3.

Figure 11. Maastrichtian deep circulation (3000 m) in (A) the eastern Neotethyan and Indian Oceans and (B) the southwestern Pacific Ocean. Orange arrows represent major deep current systems in the eastern Neotethyan and Indian Oceans and southwestern Pacific Ocean. Purple contours represent regions of deep waters formation (contour 500 m). Section A-B defines the Indonesian section of Table S1. (C) Fluxes of water across the Indonesian section over the whole water column.

Figure 12. Surface, intermediate and deep ocean temperature difference (°C) between the sensitivity experiments and the Maastrichtian simulation.

Figure 13. Cenomanian and Maastrichtian ε_{Nd} compilation modified from Moiroud et al. (2016), with few additions (Tables S3 and S4). The ε_{Nd} values at each site are averaged between 100 Ma and 90 Ma for the Cenomanian and between 75 Ma and 65 Ma for the Maastrichtian. Site numbers are shown for clarity.

Figure 14. Cenomanian ocean circulation in (A) the northern Neotethyan Ocean at 1500 m depth, (B) the North Atlantic Ocean between 0 and 500 m depth and (C) the North Atlantic Ocean between 1500 and 2000 m depth. Orange contours represent major pathways of water masses. Purple contours are the maximum winter MLD (500 m contours).

Figure 15. Deep Neotethys Seaway deep ocean circulation in the northern Indian and Neotethys Oceans at (A) 3000 m depth and (B) 2500 m depth. Orange contours represent major pathways of water masses.

Figure 16. Surface, intermediate and deep ocean temperature difference (°C) between the 2x CO_2 Maastrichtian and Cenomanian simulations.